General comment:

The ACP special issue topic is "Anthropogenic dust and its climate impact" Is there some distinction that you can make between light absorbing iron compounds (or absorption in general) in natural mineral dust aerosol versus dust aerosol from soils that have been anthropogenically disturbed or affected?

It is a very good question. As we known that the wind-blown dust which generally occurs from natural processes is commonly severe in arid or semi-arid areas (e.g. desert, Gobi and alluvial deposits), but agricultural activities that disturb the soil can greatly increase the frequency and amount of wind-blown dust. Moreover, the anthropogenic dust also includes the fugitive dust from road and non-road (such as mining and building).

To our knowledge, the light absorbing iron compounds in natural mineral dust is hard to distinct with dust aerosol from anthropogenically disturbed soils (such as grassland and cropland) by the laboratory analysis. More recently, we have developed and verified a new numerical dust model which could simulate the dust emission progress over the anthropogenically disturbed cropland and grassland (Zhang et al. 2015). Once we taken the soil mineralogical distribution data (include hematite and goethite, till now, the only datasets are from Nickovic et al. (2012) and Journet et al. (2014)) into our modeling, we will calculated the effects of anthropogenic dust on optical properties and radiative forcing. However, these modeling results are also hard to be validated. In fact, coupling the soil and emitted dust mineralogy into dust model is a new development direction to accuracy evaluates the climate impact of dust. In ACPD and ACP, Scanza et al. (2015) has modeled dust as component minerals in the Community Atmosphere Model, and Perlwitz et al. (2015) has predicted the mineral composition of dust aerosols based on the brittle fragmentation theory. However, we are opposing to the latter one and the brittle fragmentation theory in the interactive discussion progress, more details in http://editor.copernicus.org/index.php?_mdl=msover_md&_jrl=10&_lcm=oc108lcm109w&_acm=get_comm_sup_file&_ms=28358&c=85559&salt=1619220327230502394. During the past two years, our research group had carried out the field and wind tunnel experiments to building the mathematical relationships between the threshold wind velocity, soil mineralogical composition and entrained dust mineralogy (XRD and SEM-EDX), and dust size distribution over different land use types (desert, Gobi, grassland and cropland), and will couple them into our WRF-CMAQ-FENGSHA model in the future two years.

As we mentioned in our manuscript that ten of 16 known iron oxides, hydroxides and oxide-hydroxides are known occur in natural rock-forming minerals. Another six types of high-iron particles are from anthropogenically industrial activities. And these high-iron particles in fugitive dust are easy to be identified, because of their spherical morphology which formed during the combustion. However, we also know very little to the optical properties of these particles.

Journet, E., Balkanski, Y., and Harrison, S. P.: A new data set of soil mineralogy for dust-cycle

modeling, Atmos. Chem. Phys., 14, 3801–3816, doi:10.5194/acp-14-3801-2014, 2014.
Nickovic, S., Vukovic, A., Vujadinovic, M., Djurdjevic, V., and Pejanovic, G.: Technical Note: High-resolution mineralogical database of dust-productive soils for atmospheric dust modeling, Atmos. Chem. Phys., 12, 845–855, doi:10.5194/acp-12-845-2012, 2012.
Perlwitz. J. P., Pérez Garcá-Pando, C., Miller, R. L.: Predicting the mineral composition of dust aerosols–Part 1: Representing key processes, Atmos. Chem. Phys. Discus., 2015, 15(3): 3493-3575.
Scanza, R. A., Mahowald, N., Ghan, S., Zender, C. S., Kok, J. F., Liu, X., Zhang, Y., and Albani, S.: Modeling dust as component minerals in the Community Atmosphere Model: development of framework and impact on radiative forcing, Atmos. Chem. Phys., 15, 537–561, doi:10.5194/acp-15-537-2015, 2015.
Zhang, X.L., Zhou, Q.Q., Chen, W.W., Wang, Y.Y., Tong, D. Q.: Observation and modeling of black soil wind-blown erosion from cropland in Northeastern China, Aerolian Research, doi: 10.1016/j.aeolia.2015.07.009, 2015.

Line 129

I did not see that the acronym IDAD was defined. Please spell it out once.

The related text has been revised as “the Aerosol Refractive Index Archive (ARIA) of Oxford University”.

Line 208

Patterson and Gillette may have called this an accumulation mode but that does not fit the present concept of accumulation mode in aerosol science. Dropping that word does not detract from your discussion.

We have revised it and dropping this word.

Line 252

Define N, i.e. .... particle number concentration N = ...

We have revised as “for particle number concentration N=1”

Line 404

Briefly explain the inversions. I assume Koven and Fung; Formenti et al. are the references for the inversion procedure.

Yes, Koven and Fung (2006) and Formenti et al. (2014a) are the references for the inversion methods and comparisons with observed result from the AERONET.

Line 417

Explain what you mean by “advected dust aerosol”. This condition would seem to be dependent on location.

As English is not my native language, and I have corrected as “the transported dust aerosol”

Line 726

Put the reference to Köhler after Krekov.

We have revised it.

The authors greatly appreciate the constructive comments from Prof. Yves Balkanski. The reviewer pointed out that this paper could have come to even more robust conclusions with some more works. The reviewer maintains that this paper is interesting and deserve after a few improvements and corrections.

We carefully revised our manuscript in a number of locations in response to the reviewer's comments. The specifics are listed below.

This manuscript presents the importance that iron-oxides have to determine optical properties of dust. It shows how small variations of these oxides translate into large variations of the absorbing properties of dust. The authors provide a good review of the refractive indices of hematite and goethite, they then try to infer from measurements of total iron and or free-iron the range of hematite and possibly of goethite. From a proposed size distribution of dust, they study different mixing rules to document how optical parameters vary as a function of wavelength. Interestingly they show how these mixtures compare with the optical properties of pure illite as a proxy of dust without any iron-oxide. In itself, the paper is interesting and deserve after a few improvements that I propose below before being published.

1) **The authors claim that goethite has not been quantified in dust. They oversaw a reference that they cite that just did that, the mineralogical database of Journet et al. (2014) provide a quantification of hematite and goethite in soils and also as these minerals are transported in the atmosphere. The authors could have more relied on that work to narrow down the range of iron-oxides that they study (they use 0%, 2.5%, 5.0% and 7.5% by mass as study cases).**

Hematite and goethite is the major iron-minerals in airborne dust. By the regular filter sampling method, dust aerosol with the microgram mass on the filter is obtained. However, till now, the abundance of goethite in dust on filters is hard to be quantified by the laboratory analysis, such as PIXE, ICP, SEM-EDX. With the analysis of DRS, the ratio of goethite/hematite could be detected. More recently, XANES and extended X-ray absorption fine structure (EXAFS) were also used to study the specific mineral phases of iron oxides in dust, but these technologies could also not fix the abundance of goethite. Fortunately, Journet et al. (2014) provide a quantification of hematite and goethite in soils, this database could be used in dust models. The content variations during the dust emission and transport progresses are still unknown, but the study of Journet et al. (2014) could be cited as the upper limit for hematite and goethite in our study.

Journet et al. (2014) reported that the total elemental iron content of the clay fraction ranges between 0 and 15 % (in their Figure 7a), which is consistent with our summary for total iron. Thus, we cited this study in paragraph 1 line 13 of Page 5632.

In paragraph 1 line 8-10 of page 5623, we revised "hematite" as "hematite and goethite".

As Journet et al. (2014) reported that the hematite content in the clay fraction is usually < 1.5 % but reaches 5% in some regions, and even more than 5% in southern Brazil/northern Argentina. Goethite occurs in both the clay- and silt-sized fractions

and the content ranges from 0 to 15%. Actually, this modeling has underestimated the optical effects of goethite. However, the limited and discontinuous refractive indices of goethite have constrained the evaluation of the effects of specific compositions of goethite and hematite to dust optical properties and solar balance. Thus, we only set different abundance (0%, 2.5%, 5.0% and 7.5%) for hematite in the sensitive modeling. In order to further illustrate this question, we add "Due to the limited and discontinuous refractive indices of goethite, this setting may underestimate the actual optical effects of goethite in dust aerosol." to the end of line 16 in page 5635.

2) **A thorough review of the single scattering albedo (SSA) measured for dust during campaigns or inferred from AERONET measurements would have helped the authors show that having more that 5% of iron-oxides by mass could hardly be reconciled with the SSA measured for dust in the absence of black carbon (BC).**

We agree to the reviewer. A very good advice for this paper, we carefully reviewed on the reported SSAs during campaigns or inferred from AERONET measurements and satellite retrieves, and list them on Figure 4b. The measured results for dust mixed with BC were excluded during our review progress, such as the results from the campaign of AMMA. More detailed data were listed in Table 4 of our revised manuscript.

3) **The choice of the size distribution for dust particle size with an r0 of 0.5 and 0.7 μm and a σ of 2.0 is not well justified. Observations of dust size distribution can only be represented by at least 3 modes or more (see Osborne et al., 2008) and the authors would be better off considering several modes to infer dust properties.**

We thank the reviewer for pointing out that the need for further considering several modes to infer dust optical properties. We are agreeing to the presence of 3 modes or more modes for dust size distribution. In this study, we just want to fix the optical effects of iron oxides in dust aerosol, and thus we want to weaken the effects of size distribution. With reference to the OPAC, We simply choose one mode of dust to calculate the optical properties. Although this choose may be ideal with compare to the field observations and recent knowledge on size distribution of dust (Osborne et al., 2008; Mahowald et al., 2014). More recently, a modified size distribution with only one mode following brittle fragmentation theory had been published by Kok et al. (2011), but we are not agree to this theory and we are agree to the old multi-modes for dust size distribution. More detailed formula proving, please see http://editor.copernicus.org/index.php?_mdl=msover_md&_jrl=10&_lcm=oc108lcm109w&_acm=get_comm_sup_file&_ms=28358&c=85559&salt=1619220327230502394. Although previous studies on mineral dust size distributions have often attributed three to five lognormal modes, the median radii, magnitudes and standard deviations of the modes vary from study to study owing to the time-varying nature of dust particles and the source regions. In a word, one mode size distribution was chosen to simplified calculation, to compare with Sokolik et al (1999) and to help better

understanding for different readers.

With considering the advices of (2) and (3), we reviewed the reported values by several dust campaigns and AERONET observations, and then compared them with the calculated SSA curve in Figure 4b. It is shown that the SSAs were mostly ranged in 0.95-0.99 from the observation during different campaigns, but much lower (0.944-0.95) for the AERONET which cannot exclude the presence of black carbon with higher absorbing. Our calculated result could consistent with the higher part (0.97-0.99) of measured SSAs, but higher than the lower part (0.95-0.97) due to the effect of coarse particles during different dust campaigns. It is hard to compare the calculated the SSAs with measured values by considering the varied median radii, magnitudes and standard deviations of the modes, and even illustrated them in the same figure.

Mahowald N, Albani S, Kok J F, et al. The size distribution of desert dust aerosols and its impact on the Earth system[J]. Aeolian Research, 2014, 15: 53-71.

Kok J F. A scaling theory for the size distribution of emitted dust aerosols suggests climate models underestimate the size of the global dust cycle[J]. Proceedings of the National Academy of Sciences, 2011, 108(3): 1016-1021.

Minor Points:

In the abstract you mention the 'climate forcing' of dust, strictly speaking it is better to refer to it as a climate perturbation as the majority of the dust in the column is from natural sources.

We have corrected the 'climate forcing' as 'climate perturbation' in the abstract.

Page 3, lines 18 to 20: you could explain better that the radiative perturbation of dust has a positive of negative sign depending mostly on: underlying surface albedo, particle size distribution and mineralogy (see Liao and Seinfeld, 1999 and Claquin et al., 1998).

We have revised as ' However, these effects can lead to either positive or negative net radiative perturbation depending mostly on the underlying surface albedo, vertical profile (optical depth and height of dust layer), particle size distribution and mineralogy (Liao and Seinfeld, 1998; Calquin et al., 1999).'

Claquin T, Schulz M, Balkanski Y J. Modeling the mineralogy of atmospheric dust sources[J]. Journal of Geophysical Research: Atmospheres (1984–2012), 1999, 104(D18): 22243-22256.

Liao H, Seinfeld J H. Radiative forcing by mineral dust aerosols: sensitivity to key variables[J]. Journal of Geophysical Research: Atmospheres (1984–2012), 1998, 103(D24): 31637-31645.

Page 5, line 10: contrary to what is stated, Journet et al. (2014) provide the goethite fraction (in mass) globally and by regions for both the clay and silt fraction of dust.

We have corrected as 'More recently hematite and goethite has been taken into account interactively in global climate simulations due to the availability of global

mineralogical distribution maps (Nickovic et al., 2012; Journet et al., 2014).'.

Page 9, line 4: The reference LG1985 is not defined in the text and I could not find it in the reference list.

We are sorry for error writing the "QE1985" as "LG1985", and have corrected it as "QE1985"in the manuscript.

Page 16 lines 20-24 state: '' Based on the above reported results, we conclude that the iron-oxides account for approximately half of the mass of elemental Fe and for between 2 and 5% of the dust mass. Most of them are composed of goethite, representing between 50 and 75% of the iron oxide mass." How do you then justify the choice of your 4 cases : 0, 2.5, 5.0 and 7.5% hematite lines 14-17 page 17. Please indicate very clearly whether these fracions refer to mass fractions or volume fractions (since when you work with optical parameters you consider volume).

The abundance of hematite was used to calculate the effective complex refractive indices for dust by the volume mixing method, the Bruggeman approximation and the Maxwell–Garnett approximation. For the volume mixing method, the simplest way to sum up the refractive indices of its individual constituents weighted by their volume (or mass). The volume fractions of hematite that converted from mass fractions with using the density of hematite (5.3 g/cm3) and illite (2.75 g/cm3) (Moosmüller et al., 2012). Then the volume fractions of hematite were used in above three methods.

In order to very clearly indicate this question, we have added "Using the density of hematite (5.3 g/cm3) and illite (2.75 g/cm3), volumetric hematite fraction was converted from the mass hematite fraction to calculated the effective complex refractive indices for dust." to the end of line 17 of page 5635. The 4 cases were also further explained as 0, 2.5, 5.0 and 7.5% hematite in mass in lines 14-17 of page 5635.

Page 19 lines 14 to 17. '' This is explained by Fig. 4b where the two datasets have the same optical scattering and absorbing properties for $\lambda < 0.55$ µm but the dataset of QE1985 leads to higher optical absorption for $\lambda > 0.55$ µm.". Check the Figure you refer to, I could not reach your conclusion by looking at Figure 4b.

We have rechecked the figure and make sure that we refer to Figure 4b. In order to check the spectral difference of SSA between QE1985 and LG1988 and simple to read figure 4b, we only drawn the dashed purple line for LG1988_7.5% with compare the solid pink line for QE1985_7.5%. Similar spectral features of other abundances for hematite and were omitted in Figure 4b. With the comparison between the dashed purple line and the solid pink line, we got that "the two datasets have the same optical scattering and absorbing properties for $\lambda < 0.55$ µm but the dataset of QE1985 leads to higher optical absorption for $\lambda > 0.55$ µm".

Page 21 line 27. The sentence that starts with 'Therefore, the employment of

refractive indices. . .' is akward, replace it with 'Therefore, the use of refractive indices. . .'
We have revised it.

Pages 21 and 22 have been hastily written, try to improve the text for these 2 pages.
We have extensively improved the text from 5639-5640.

The conclusions might need some work to extract better your main findings.
We have reorganized the conclusions in the revised manuscript.

We thank the anonymous referee #2 for his/her valuable comments to the manuscript and the constructive suggestions for improving the presentation quality. We have tried and addressed these comments at the best of our possibilities. Below, we explain how the comments and suggestions are addressed (responses in blue color).

Referee #2

I first would like to apologize with authors and the editor for the delay in submitting this review. This manuscript present a sensitivity study of the optical properties of dust mixtures including iron oxides to the values of their refractive index, to their state of mixing within the dust matrix and to the shape. The topic is surely of interest as iron oxides control the light-absorbing properties of mineral dust which ultimately control their direct and semi-direct radiative effect. Pointing out to the discrepancies in the current state of knowledge is surely beneficial in promoting new research in the area.

Nonetheless, the paper presents various weaknesses that must be addressed before considering publication. In particular, the paper presents a very large number of references. However, there is a great confusion and a great deal in simplification in their use, leading to misleading discussion and conclusions. The authors should pay more attention in separating research results that 1/ dealt with dust in the aerosol phase to those that dealt with dust in soils 2/ dealt with standard material (synthetic minerals, proxies.) to those that dealt with dust in the aerosol phase.

We agree to the referee that a very large number of references are presented in this paper, and some of them had been cited unreasonable and even in error. We have rechecked all references and revised them. We admit that we just want to fix the upper limit for iron oxides in dust aerosol. However, we know very little to how many iron oxides within dust in the aerosol phase are originated from the iron oxides within dust in soil. As the iron oxides emitted from the soil dust, and thus, we did not considering the specific forms of iron oxides in our original manuscript. After reading the suggestion from referee #2, we fully accept this good constructive suggestion and reorganized the related paragraphs to make our revised manuscript more understandable to readers, and make note of the changes we have made to the discussion paper.

Some specific comments:

a) **Size distribution (paragraph 2.2): a model of size distribution is proposed. The authors do not consider a coarse mode, whereas, by their own admission, mineral dust is characterized by one. As a matter of fact, the coarse mode of mineral dust can contribute to lower the single scattering albedo of dust. What is the competition with the value of the complex refractive index of the iron oxides?**

The editor and both two reviewer have pointed out the setting of size distribution is not well justified. We are agreed to the 3 modes or more modes for dust size distribution. In this study, we want to fix the optical effects of iron oxides in dust aerosol, and thus we want to weaken the effects of size distribution. With reference to

the OPAC, We simply choose one mode of dust to calculate the optical properties. Although this choose may be ideal with compare to the field observations and recent knowledge on size distribution of dust (Osborne et al., 2008; Mahowald et al., 2014). More recently, a modified size distribution with only one mode following brittle fragmentation theory had been published by Kok et al. (2011), but we are not agree to this theory and we are agree to the old multi-modes for dust size distribution. More detailed formula proving, please see http://editor.copernicus.org/index.php?_mdl=msover_md&_jrl=10&_lcm=oc108lcm109w&_acm=get_comm_sup_file&_ms=28358&c=85559&salt=1619220327230502394. Although previous studies on mineral dust size distributions have often attributed three to five lognormal modes, the median radii, magnitudes and standard deviations of the modes vary from study to study owing to the time-varying nature of dust particles and the source regions. In a word, one mode size distribution was chosen to simplified calculation, to compare with Sokolik et al (1999) and to help better understanding for different readers.

With considering the advices of (2) and (3), we reviewed the reported values by several dust campaigns and AERONET observations, and then compared them with the calculated SSA curve in Figure 4b.

What is the competition of coarse size for dust with the value of the complex refractive index of the iron oxides? Figure 4b is shown that the SSAs were mostly ranged in 0.95-0.99 from the observation during different campaigns, but much lower (0.944-0.95) for the AERONET which cannot exclude the presence of black carbon with higher absorbing. Our calculated result could consistent with the higher part (0.97-0.99) of measured SSAs, but higher than the lower part (0.95-0.97) due to the effect of coarse particles during different dust campaigns. It is hard to compare the calculated the SSAs with measured values by considering the varied median radii, magnitudes and standard deviations of the modes, and even illustrated them in the same figure.

Mahowald N, Albani S, Kok J F, et al. The size distribution of desert dust aerosols and its impact on the Earth system[J]. Aeolian Research, 2014, 15: 53-71.

Kok J F. A scaling theory for the size distribution of emitted dust aerosols suggests climate models underestimate the size of the global dust cycle[J]. Proceedings of the National Academy of Sciences, 2011, 108(3): 1016-1021.

b) Goethite/hematite ratios: the authors have to distinguish between quantitative (such as those presented in Formenti et al. 2014 using X-ray absorption) and qualitative measurements such as those presented in Formenti et al. 2008, Lafon et al. (2006) and Klaver et al (2011) using diffuse reflectance spectroscopy.

Thanks for the suggestion. The speciation of iron oxides in dust aerosol could be identified by X-ray absorption (XAS) in the Fe K range: XANES (X-ray absorption near-edge structure) and EXAFS (extended X-ray absorption fine structure). XAS spectroscopy is based on the analysis of the position and shape of the K pre-edge and edge peaks, depending on the oxidation state of iron but also on the atomic position of the neighbouring atoms, mostly O+ and OH−. The XANES

analysis can identify also other Fe-minerals depending on the inflection points of their absorption spectra, such as magnetite. The position of the inflection points is very similar for goethite, hematite and magnetite; the relative proportions of the peaks in the absorption spectra are different. It should not be forgotten than, as discussed by Lazaro et al. (2008), magnetite accounts for less than 7% of the total iron in aerosol dust samples. This is of the same order of magnitude that the errors of the fit taking into account the differences between the minerals in their standard and in their real forms. The quantification of the Fe status was based on the analysis of five standards of Fe(III)-bearing minerals which can be found in mineral dust (Formenti et al., 2014b). The final obtained result is quantitative; the ratio of goethite/hematite is also quantitative.

DRS use the characteristic bands of hematite and goethite in the visible absorption spectrum at around 565 nm and 435 nm, respectively. Moreover, by taking the second derivative of the diffuse reflectance signal, it is possible to determine quantitatively a relative mass fraction of hematite and goethite (Lafon et al., 2006). Thus, the reported results from diffuse reflectance spectroscopy are also quantitatively relative ratios for goethite/hematite. So we compiled the results from XAS with DRS in Table 3 of our manuscript.

Lazaro, F. J., et al., The speciation of iron in desert dust collected in Gran Canaria (Canary Islands): Combined chemical, magnetic and optical analysis, Atmospheric Environment 42 (2008) 8987–8996

Lafon, S., Sokolik, I., Rajot, J., Caquineau, S., and Gaudichet, A.: Characterization of iron oxides in mineral dust aerosols: Implications for light absorption, J. Geophys. Res., 111, D21207, doi:10.1029/2005JD007016, 2006.

c) Abundance of iron and iron oxides (paragraph 3.2.2) c.1/Page 15, lines 20 on. Not all the references you mention used XRD to quantify the iron oxides c.2/Page 16, line 9. Formenti et al. 2014 did NOT use diffuse reflectance spectroscopy to obtain the hematite-to-goethite ratio.

Response to C.1:

We carefully recheck the references, and found that:

Bernabé et al. (2005) had used XRD to identify the mineralogy of deposited atmospheric dust and dust aerosol, and reported that hematite presented only within the sedimentable dust particles but without reported on the abundance of hematite. Thus, we delete this reference from our citation.

All other cited references had used XRD to quantify the iron oxides, and we simply introduced as following:

Shi et al. (2005) quantified the abundance of hematite (0.9% in mass) in PM10 sample that collected during an Asian dust storm.

Linke et al. (2006) reported that no detectable iron oxides phases in Cairo samples and ~0.2 wt-% of goethite in the Agadez sample and 0.6±0.1 wt-% of hematite in the Morocco sample.

Kandler et al. (2009) reported their quantified results (1 wt%) for hematite in Morocco dust sample based on XRD with RIR method.

Lawrence et al. (2010) illustrated the abundance (0.1-0.8 wt%) of goethite in deposited dust of Colorado sample based on XRD with the RockJock software.

Klaver et al. (2011) measured the mass content (0.6-1.8 wt %) of iron oxides in transported dust samples collected by aircraft during GERBILS campaign and reported their detailed results in

Table V of their research paper.
Wagner et al. (2012) shown that the iron oxide content (hematite and/or goethite) does not exceed 1 wt % in entrained dust aerosol from soil dust samples collected during SAMUM-1 campaign. In contrast, the Burkina Faso sample collected during AMMA campaign shown a very high content of iron oxides (15 wt %) with a hematite to goethite ratio of 4:1. All samples were analyzed by XRD with the RIR method.
Finally, we add the new XRD analysis of Formenti et al. (2014b).

Formenti, P., Caquineau, S., Desboeufs, K., Klaver, A., Chevaillier, S., Journet, E., and Rajot, J.: Mapping the physic-chemical properties of mineral dust in western Africa: mineralogical composition, Atmos. Chem. Phys., 14, 10663–10686, doi:10.5194/acp-14-10663-2014, 2014b.

Response to C.2:
We are sorry for this obviously error ciation, and this reference had been deleted in revised manuscript.

Furthermore, Formenti et al. (2014) in line 4 of page 5635 is also error cited due to our editing for the list of references. The correct reference is:

Formenti, P., Caquineau, S., Desboeufs, K., Klaver, A., Chevaillier, S., Journet, E., and Rajot, J.: Mapping the physic-chemical properties of mineral dust in western Africa: mineralogical composition, Atmos. Chem. Phys., 14, 10663–10686, doi:10.5194/acp-14-10663-2014, 2014b.

Following is our revised manuscript in PDF format.

What's the real role of iron-oxides in the optical properties of dust aerosols?

Xuelei Zhang[1, 2], Guangjian Wu[2], Chenglong Zhang[3], Tianli Xu [2, 4], Qinqian Zhou[1]

[1]*Key laboratory of Wetland Ecology and Environment, Northeast Institute of Geography and Agroecology, Chinese Academy of Sciences, Changchun,130102, China*

[2] *Key Laboratory of Tibetan Environment Changes and Land Surface Processes, Institute of Tibetan Plateau Research, CAS Center for Excellence and Innovation in Tibetan Plateau Earth System Sciences, Chinese Academy of Sciences, Beijing 100101, China*

[3] *Research Center for Eco-Environmental Sciences, Chinese Academy of Sciences, Beijing, 100085, China*

[4] *University of Chinese Academy of Sciences, Beijing 100049, China*

Correspondence to: X. L. Zhang (zhangxuelei@neigae.ac.cn) and G. J. Wu (wugj@itpcas.ac.cn)

Abstract:

Iron oxides compounds constitute an important component of mineral dust aerosol. Several previous studies have shown that these minerals are strong absorbers at visible wavelengths and thus that they play a critical role in the overall climate ~~forcing~~ perturbation caused by dust aerosol. When compiling a database of complex refractive indices of possible mineral species of iron-oxides to study their optical properties, we found that uniformly continuous optical constants for a single type of iron-oxides in the wavelength range between 0.2 μm and 50 μm is very scarce and that the use of hematite to represent all molecular or mineral iron-oxides types is a popular hypothesis. However, the crucial problem is that three continuous datasets for complex refractive indices of hematite are employed in climate models, but there are significant differences between them. Thus, the real role of iron-oxides in the optical properties of dust aerosols becomes a key scientific question, and we address this problem by considering different refractive indices, size distributions, and more logical weight fractions and mixing states of hematite. Based on the microscopic observations, a semi-external mixture that employs an external mixture between Fe-aggregates and other minerals and partly internal mixing between iron-oxides and aluminosilicate particles is advised as the optimal approximation. The simulations demonstrate that hematite with a spectral refractive indices from Longtin et al. (1988) shows approximately equal absorbing capacity to the mineral illite over the whole wavelength region from 0.55 μm to 2.5 μm, and only enhances the optical absorption of aerosol mixture at $\lambda<0.55$ um. Using the dataset from Querry (1985) may overestimate the optical absorption of hematite at both visible

and near-infrared wavelengths. More laboratory measurements of the refractive index of iron-oxides, especially for hematite and goethite in the visible spectrum, should therefore be taken into account when assessing the effect of mineral dust on climate forcing.

1. Introduction

Iron oxides in dusts are now identified as being important component for a number of climatic, environmental and biological processes. Over the past decade, iron-oxide minerals have been shown to be able to strongly absorb solar radiation (Tegen et al., 1997; Sokolik and Toon, 1999; Lafon et al., 2004; Qin and Mitchell, 2009; Redmond et al., 2010), and thus have a direct impact on the Earth's radiation balance (Balkanski et al., 2007; ~~Scanza et al., 2014;~~ Smith and Grainger, 2014; Scanza et al., 2015). Based on the ability to absorb~~–~~ acidic gases and water vapor (Baltrusaitis et al., 2007; Wijenayaka et al., 2012; Song and Boily, 2013), iron oxides also contribute to heterogeneous reactions and cloud processes (Shi et al., 2011; Dupart et al., 2012), further influencing the radiation balance. In particular, layers of dust on snow and ice cover accelerate the melting of snow and ice by diminishing the surface albedo (Painter et al., 2010; Ginot et al., 2014) and the heat-absorbing properties of iron oxides in these dust layers can add to this effect (Kaspari et al., 2013; Reynolds et al., 2013; Dang and Hegg, 2014). Moreover, the deposited iron-bearing dust aerosols provide critical nutrients to marine and terrestrial ecosystems, which associated with consequential important drawdown of atmospheric carbon dioxide (Jickells et al., 2005; Shao et al., 2011; Nickovic et al., 2013). However, these effects can lead to either positive or negative net radiative forcing depending mostly on the underlying surface albedo, vertical profile (optical depth and height of dust layer), particle size distribution and mineralogy (Liao and Seinfeld, 1998; Calquin et al., 1999). This large uncertainty results from our limited knowledge of the physical, chemical and optical properties of atmospheric iron oxides on various space and time scales (Tegen et al., 1997; Sokolik et al., 2001; Formenti et al., 2011).

The element iron can be found among numerous mineralogical species, such as feldspars, clays (e.g. illite, smectite, chlorite and biotite), iron-oxides, iron-hydroxides and so on. A useful mineralogical classification frequently used in soil science distinguishes two categories of iron: (i) "structural iron" (in either the Fe(II) or Fe(III) oxidation states), trapped in the crystal lattice of aluminosilicate minerals; and (ii) iron (in the Fe(III) oxidation state), in the form of discrete oxide

or hydroxide particles (Lafon et al., 2004). According to the classical terminology of soil scientists (Sumner, 1963; Anderson and Jenne, 1970; Angel and Vincent, 1978), the latter kind of iron will be referred to as free-iron and its corresponding oxides and hydroxides as iron-oxides. Ten of 16 known iron oxides, hydroxides and oxide-hydroxides are known occur in nature, with goethite, hematite and magnetite being the most abundant as rock-forming minerals; ferrihydrite, maghemite and lepidocrocite being intermediately abundant in many locations; and wüstite, akaganéite, feroxyhyte, and bernalite being the least abundant (Cornell and Schwertmann, 2006; Guo and Barnard, 2013). Dust aerosols from arid and semi-arid regions typically contain goethite, hematite, ferrihydrite and magnetite, —and based on the mass contribution, hematite and goethite are the major components of free-iron in the atmospheric dust aerosols (Schroth et al., 2009; Shi et al., 2012; Takahashi et al., 2013). Hematite (Fe_2O_3) is very common in hot, dry soils and imparts a red color to its sediments. Goethite (α-FeOOH) is a common weathered product in soils and loesses. It occurs in moist, acidic soils (Schwertmann, 1993), and is brown to yellow in color.

Sokolik and Toon (1999) found that hematite is an especially strong absorber at ultra-violet (UV) and visible wavelengths, and it can also enhance the absorption of clay minerals and quartz through the formation of aggregates. Derimian et al. (2008) mentioned that iron oxides (primarily hematite and goethite) only affect the optical absorbing ability of aeolian dust at short wavelengths (the blue spectral region). Since the importance of hematite relative to other dust mineral components was discussed more fully in the study of Sokolik and Toon (1999), most subsequent modeling studies have assumed the iron-oxides in dust aerosols to be in the form of hematite. An opposite viewpoint was put forward, however, by Balkanski et al. (2007) who have argued that the optical absorption of dust with hematite at visible wavelengths might be lower than previous thought. The main reason is that internal mixing rule calculations with a hematite content of 1.5 volume % (or 2.8 weight %) was supposed to be representative for median dust absorption and was, as well, consistent with the AERONET measurements.

However, recent measurements on dust samples from east Asia, northern Africa and western Africa (Lafon et al., 2006; Formenti et al., 2008; Reynolds et al., 2014; Formenti et al., 2014) indicated that goethite was presented in higher concentration than hematite (i.e. the ratio of goethite to hematite is about 7:3, a result that will be detail introduced in Section 3.2.2). For dust in snow, goethite is also the dominant ferric oxide that detected by reflectance spectroscopy and

thus appears to be the main iron-oxide control on absorption of solar radiation (Reynolds et al., 2013). More recently hematite and goethite has been taken into account interactively in global climate simulations due to the availability of global mineralogical distribution maps (Nickovic et al., 2012; Journet et al., 2014), but this has been impracticable for geothite.

Furthermore, Müller et al. (2009) have measured the spectral imaginary refractive indices of hematite over the wavelengths from 590 nm to 790 nm during laboratory experiments, but these derived values are much lower than the data that employed in Sokolik and Toon (1999). The theoretical simulations of optical scattering of hematite and goethite at 470, 550, and 660 nm by Meland et al. (2011) also found that differences are apparent for hematite in both the phase function and polarization results at 660 nm where the imaginary indices from different references differ. Additionally, two studies that refer to optical properties of hematite in dust samples have also argued that the imaginary values of hematite refractive index in Sokolik and Toon (1999) are more than a factor of 2 larger than those reported by Bedidi and Cervelle (1993) and Longtin et al. (1988) at wavelengths below 600 nm (Moosmüller et al., 2012; Wagner et al., 2012).

Thus, what is the real role of iron-oxides in determining the overall impact of the optical properties of dust aerosols? This study will focus on investigating this important scientific question by considering heterogeneous optical refractive indices, mixing states and more logical abundance of iron-oxides.

2. Method and simulation

2.1 Complex refractive index

The complex refractive index (optical constant) is the most basic and significant parameter for calculating the optical properties of aerosols, but values for the optical constants of hematite in the wavelength range 0.2 to 50 μm are scarce in published references. Table 1 compiles information about the complex refractive indices of the major constituents of free-iron that we have found in the published literature. Sokolik and Toon (1999) employed the refractive indices of hematite from Querry et al. (1978), but Querry et al. (1978) mainly studied the optical constants of limestone and, as far as we can discover, do not contain any work on hematite at all. Since the publication of Sokolik and Toon (1999), studies (Höller et al., 2003; Alfaro et al., 2004; Mishra and Tripathi, 2008; Otto et al., 2009; Munoz et al., 2006; Meland et al., 2011; Wagner et al., 2012)

have misquoted the data as Querry et al. (1978) or Querry (1987) when modeling the optical properties of hematite. Actually, Querry (1987) is entitled "Optical constants of minerals and other materials from the millimeter to the UV" and gives optical constants of 29 materials, but still without referring to hematite. After careful searching, we have found that Querry (1985) has tabulated values for the refractive index ($m = n + ki$) of hematite. Moreover, Longtin et al. (1988) also reported spectral refractive indices for hematite from earlier measurements by Steyer (1974), Onari et al. (1977), Galuza et al. (1979) and Kerker et al. (1979). This dataset also has been used in modeling the contribution of hematite to the optical properties of atmospheric dust aerosols in recent studies (Klaver et al., 2011a; Köhler et al., 2011; Hansell et al., 2011). Recently, the third unpublished continuous refractive indices of hematite (named TA2005 in Table 1) from the ~~IDAD~~Aerosol Refractive Index Archive (ARIA) ~~database~~ of Oxford University have been employed in the Community Atmosphere Model (Scanza et al., ~~2014~~2015). Because this work has not been peer-reviewed and because TA2005 and QE1985 show a similar wavelength dependency, ~~–~~ we pay special attention to the differences of refractive indices between QE1985 and LG1988 in this paper. Any errors due to uncertainties in the optical constants would be directly reflected in the calculated results referred to above.

Table 1. Summary of the published complex refractive indices for major constituents of free-iron at different wavelengths (with their references).

Iron-oxide species	Wavelength (μm)	Reference source	Abbreviation
Hematite	8.3-50	Popova et al. (1973)	PV1973
Hematite	1.0-333	Onari et al. (1977)	OA1977
Hematite	0.25-0.7	Shettle and Fenn, (1979)	SF1979
Hematite	0.35-0.65	Hsu and Matijevic, (1985)	HM1985
Hematite	0.21-90	Querry (1985)	QE1985
Hematite	0.3-300	Longtin et al. (1988)	LG1988
Hematite	0.2-0.7	Gillespie and Lindberg, (1992)	GL1992
Hematite	0.2-4.5	Krekov (1992)	KE1992
Hematite	0.35-0.75	Bedidi and Cerville (1993)	BC1993
Hematite	0.1-1000	Triaud (2005)*	TA2005
Hematite	5-50	Marra et al. (2005)	MR2005
Hematite	5-2000	Glotch and Rossman, (2009)	GR2009
Hematite	0.59-0.79	Müller et al. (2009)	ML2009
Magnetite	0.21-55	Querry (1985)	QE1985
Magnetite	5-50	Mukai (1989)	MK1989
Magnetite	0.25-0.7	Gillespie and Lindberg, (1992)	GL1992

Magnetite	0.1-1000	Amaury et al. (2002)	AU2002
Magnetite	5-100	Glotch and Rossman, (2009)	GR2009
Goethite	0.45-0.75	Bedidi and Cerville, (1993)	BC1993
Goethite	8-50	Glotch and Roman, (2009)	GR2009
Wüstite	0.2-500	Henning (1995)	HN1995
Wüstite	10-500	Henning and Mutschke, (1997)	HN1997

* The data was taken from http://www.atm.ox.ac.uk/project/RI/hematite.html

Bedidi and Cervelle (1993) also presented refractive indices for hematite and goethite derived from reflectance measurements at wavelengths of 350-750 nm. Glotch and Rogers (2007) reported the optical constants of hematite, goethite and magnetite over the infrared (IR) wavelengths, and Hsu and Matijević (1985) also measured the refractive indices of hematite in the wavelengths of 350-650 nm.

Hematite is a uniaxial crystal which crystallizes in the trigonal system, whose optic axis corresponds to the crystallographic *c*-axis. Perpendicular to the *c*-axis are two radial *a*-axes. The dielectric constants of bulk hematite must therefore be measured for two principal polarizations of the incident light, namely one with the electric vector in any direction perpendicular to the *c*-axis (the so-called ordinary ray or – O ray) and the other with the electric vector along the crystalline *c*-axis (the extraordinary ray or – E ray). In this work we have calculated the average refractive indices for anisotropic hematite from all references in Table 1. The formula used is adopted from Longtin et al. (1988) and is:

$$m_{avg} = (2n_{E-ray} / 3 + n_{O-ray} / 3) + (2k_{E-ray} / 3 + k_{O-ray} / 3)i.$$

The reported values for the complex refractive index from the sources in Table 1 are markedly different, especially the imaginary part which controls the optical absorption. In order to visually demonstrate the variation of optical constants from different references, values of the real (n) and logarithmic values of imaginary parts (k) are shown in Figure 1.

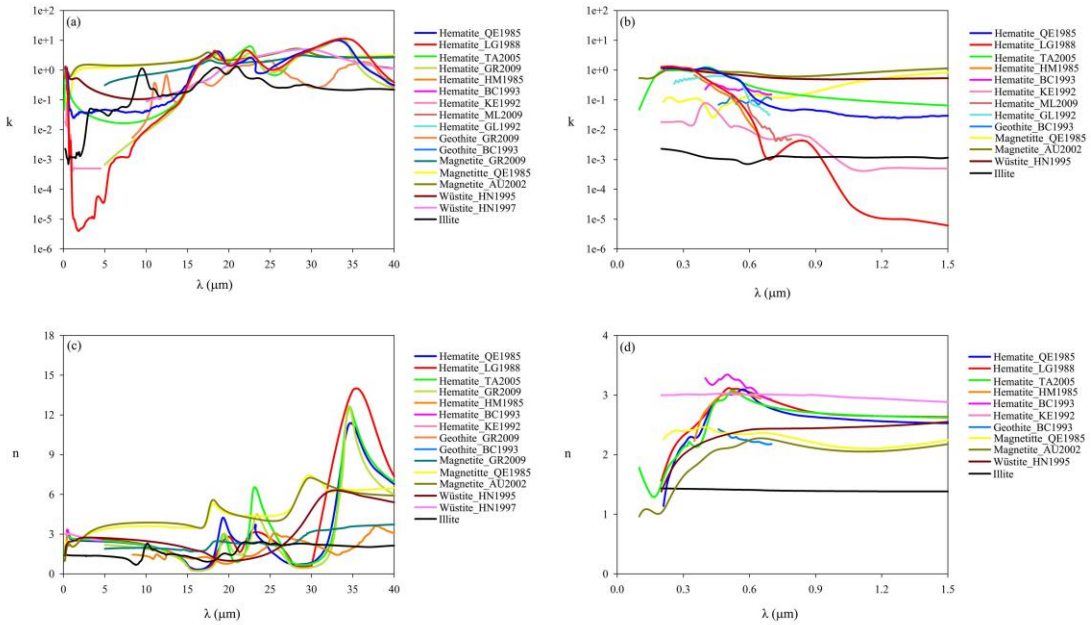

Fig. 1. Spectral distribution of the imaginary and real parts of the complex refractive index for different iron oxides from Table 1 at wavelengths of 0 to 40 μm (Panels (a) and (c)) and expanded for wavelengths of 0 to 1.5 μm (Panels (b) and (d)).

For the real part of the refractive index for iron-oxides, there is a reasonable agreement between the hematite and magnetite datasets from the different references (Figure 1c). Because the real refractive index of hematite shows large fluctuations at wavelengths longer than 18 μm due to anisotropic refraction, the agreement between the different datasets decreases at these wavelengths. For goethite we are aware of only two sets of optical constants: one at visible wavelengths from Bedidi and Cervelle (1993) and the other at IR wavelengths from Glotch and Rogers (2007), but the wavelength gap between these two datasets hampers continuity. Unfortunately, Meland et al. (2011) have checked the former dataset for goethite using simulations according to Mie and T-Matrix theories and show that it may be in error. Nevertheless, we can see that goethite has optical constants similar to hematite. The real refractive index of hematite is larger than that of magnetite at wavelengths less than 2μm, but is smaller between 2 and33 μm (Figures 1c&d).

For the imaginary part of the refractive index of iron-oxides, hematite and goethite have different optical properties at short wavelengths, both in terms of magnitude and spectral dependence (Bedidi and Cervelle, 1993). Between 460 and 700 nm the imaginary part of the complex refractive index (representing absorption) of goethite is up to 3 times smaller than that of hematite. As a consequence, the proportions of hematite and goethite in mineral dust can

potentially change the magnitude and the spectral dependence of shortwave absorption of mineral dust. However, the limited and discontinuous refractive indices of goethite have constrained the evaluation of the effects of specific compositions of goethite and hematite to dust optical properties and solar radiation balance over broader wavelength ranges.

From Figure 1a, we clearly see that the k values for hematite from QE1985 and from LG1988 show significant differences for wavelengths between 650 nm and 15 μm. These differences are present at visible wavelengths and disappear at ultraviolet wavelengths, but the two datasets have similar trends at UV and visible wavelengths (Figure 1b). Note that the hematite optical constants vary dramatically across the visible wavelengths. In particular, the imaginary part of the index for hematite shows a sharp decrease with increasing wavelength in the red. As a consequence there is a large variability in the imaginary refractive index values for hematite taken from different published references, particularly at 2 μm where the ~~imaginary index~~ values from different sources differ by a factor of 8600. Thus, this study firstly focuses on what will be the result if these heterogeneous optical constants of hematite are used as input for the calculation of radiation transfer models.

2.2 Particle size distribution

Size distribution is another important factor that affects the optical properties of particles. Because Sokolik and Toon (1999) has employed the refractive index dataset for hematite from ~~LG1985~~ QE1985 to calculate the radiative properties, we adopt here the same particle size distribution but with the refractive index dataset for hematite from LG1988 to compare our results with Sokolik and Toon (1999). The lognormal distribution is applied to dust aerosols:

$$n_n(\ln r) \equiv \frac{dN}{d\ln r} = \frac{N_0}{\sqrt{2\pi}\ln\sigma}\exp\left[-\frac{1}{2}\left(\frac{\ln r - \ln r_0}{\ln\sigma}\right)^2\right],$$

where r_0 is the median radius, σ is the geometric standard deviation, and N_0 is the total particle number density of the component in particles per cubic centimeter.

In order to compare with the results of Sokolik and Toon (1999), the optical properties of minerals are calculated on the assumption that they have one size mode but varying median radius. The particle size modes are selected as r_0 = 0.5 and 0.7 μm, and σ = 2.0. The size mode with

median radius r_0 = 0.5 μm is believed to be representative of the particle size distribution of the long-lived, long-distance-transport ~~accumulation~~ mode of airborne dust (Patterson and Gillette, 1977; Arimoto et al., 1997). The larger r_0 is representative of a particle size mode which occurs near the dust source (Gomes and Gillette, 1993). In reality, the size distribution of dust aerosols can have one or several modes, characterized by a specific composition (Mahowald et al., 2013).

2.3 Theoretical simulations

Images from scanning electron microscopy (SEM) reveal non-spherical, irregular and compact shapes of the dust particles (Figure 3), but Otto et al. (2009) and Klaver et al. (2011b) have shown that spherical/non-spherical differences only influence the single scattering albedo by less than 1%. Meland et al. (2011) have also shown that moderate departures from spherical shape are relatively unimportant in determining the scattering matrix for particles with high refractive index values, such as hematite. Therefore, we expect the aerosol asphericity to have a negligible impact on our calculated results of optical properties and subsequent calculations using the Mie theory (which assumes a spherical morphology for the dust particles).

There are several different computer codes that can be used to compute optical properties for a lognormal particle size distribution. The theoretical light scattering simulations in this paper have used the MieTab software. MieTab uses a FORTRAN code with continued fraction modification produced by W. J. Lentz from the Mie code originally developed by Dave and Center (1968). This modified code can be obtained from http://diogenes.iwt.uni-bremen.de/vt/laser/codes/ddave.zip. In order to validate the accuracy of MieTab, we firstly compared it with a double precision Lorenz-Mie scattering code and a double precision T-Matrix code for a lognormal particle size distribution from Mishchenko et al. (2002). The double precision Lorenz-Mie and T-Matrix codes are available from http://www.giss.nasa.gov/staff/mmishchenko/t_matrix.html.

In addition to the wavelength dependent optical constants and the size distribution, the T-Matrix theory also requires assumptions about the particle shape. In this work we use an aspect ratio of 1.000001 to represent a spherical particle shape, because use of an aspect ratio exactly equal to 1 causes computational overflow in some cases. The calculated results from the three codes at different wavelengths and complex refractive indices for the same size distribution are

listed in Table 2. The good agreement of the results from the three codes demonstrates that the possibility of computational error affecting the interpretation of the calculated optical properties of iron-oxides can be neglected.

Table 2. Comparison of simulated optical properties between MieTab, Lorenz-Mie and T-matrix methods.

Wavelength	550 nm			633 nm			1060 nm		
$m=n+ki$	n=3.102, k=0.0925			n=3.007, k=0.00974			n=2.66, k=0.00003		
Code type	MieTab	T-matrix	Lorenz-Mie	MieTab	T-matrix	Lorenz-Mie	MieTab	T-matrix	Lorenz-Mie
Q_{ext}	2.0950	2.1332	2.1637	2.1440	2.1917	2.2585	2.3250	2.5042	2.0226
Q_{sca}	1.2640	1.3284	1.3233	1.8500	1.9048	1.9587	2.3240	2.5033	2.0216
Q_{abs}	0.8310	0.8048	0.8404	0.2940	0.2870	0.2998	0.0010	0.0009	0.0010
ω_0	0.6033	0.6227	0.6116	0.8629	0.8691	0.8673	0.9996	0.9996	0.9995

3. Results and discussion

3.1 Basic optical properties

We focus here on modeling the spectral optical properties of iron-oxides which are needed for climate modeling: the volume extinction coefficient β_{ext} (which is the sum of the scattering coefficient β_{sca} and the absorption coefficient β_{abs}), the single scattering albedo ω_0, and the asymmetry parameter g (a cosine weighted integral of the scattering phase function). This set of parameters allows the calculation of radiation forcing in most climate models. Figure 2 shows calculated optical parameters for hematite (with complex refractive indices from QE1985 and LG1988) and illite with varying median radius at solar and infrared wavelengths. The volume total extinction coefficients β_{ext} have been normalized as β_{ext}^{*} for particle number concentration $N=1$ cm^{-3}.

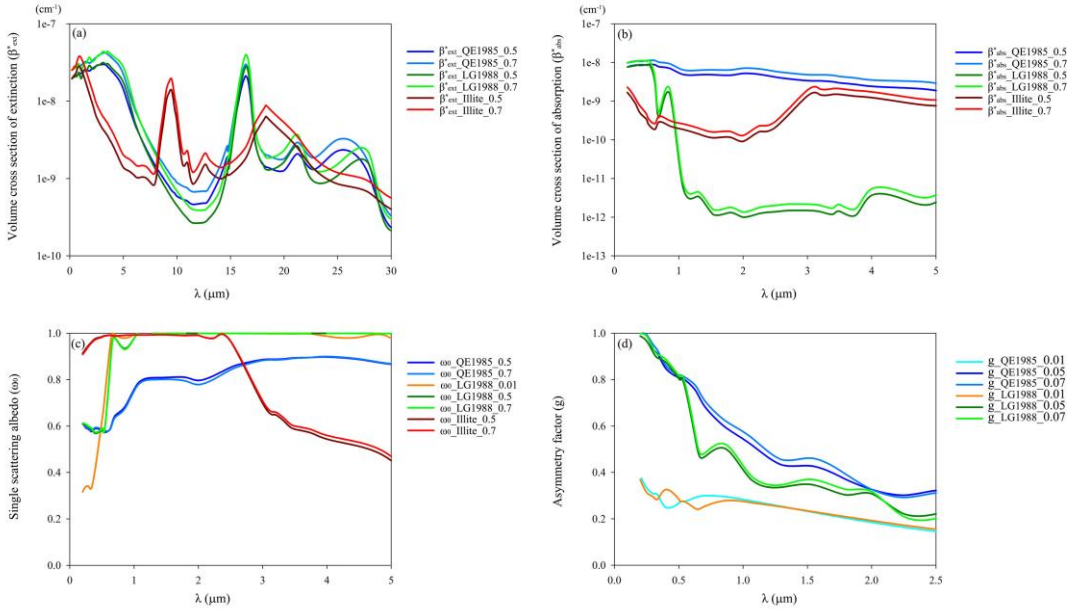

Fig. 2. The calculated spectral optical properties for hematite, goethite and illite with different complex refractive index and size distribution. (a) Volume cross section of extinction, (b) Volume cross section of absorption, (c) Single scattering albedo and (d) Asymmetry factor

Figure 2a and Figure 2b demonstrate how the normalized spectral extinction coefficient and the normalized spectral absorption coefficient vary due to the differences in the refractive indices and median radius of the minerals. As shown in Figure 2a, β_{ext}^{*} for hematite has a spectrum which is clearly distinguishable from that for illite at UV, visible and IR wavelengths. One point should be noted: hematite has a lower normalized spectral extinction coefficient than illite at wavelengths less than 1.3 μm, which means that hematite has a weaker optical extinction capacity than illite at these wavelengths. In the IR region, the spectral features of hematite in β_{ext}^{*} show large differences in volatility, and mimic the features in the refractive index of hematite. The magnitude of β_{ext}^{*} depends on the parameters of the particle size distribution.

Figure 2b shows the equivalent normalized spectral absorption coefficient for hematite from QE1985 and LG1988 at wavelengths less than 5 μm. The normalized absorption coefficient of hematite from QE1985 is about 100 times larger than that for illite at both visible and near-IR wavelengths, but the normalized absorption coefficient for hematite from LG1988 has larger values than those for illite at wavelengths less than 1 μm and about 100 times smaller values than

those for illite at wavelengths between 1 μm and 5 μm. If we adopt the complex refractive indices of QE1985, the calculated absorption coefficient of hematite indicates that hematite is an especially strong absorber at UV and visible wavelengths. Conversely, the calculated absorption coefficient of hematite using LG1988 data suggests that hematite is an important aerosol component only for short-wavelength absorption. Considering the whole region from 0.2 μm to 5 μm, hematite with complex refractive indices from LG1988 has an approximately equal absorbing capacity to that of illite.

Figure 2c illustrates the single scattering albedo of hematite and illite at wavelengths between 0.2 μm and 5 μm for different particle size distributions. The single scattering albedo of hematite is about 0.6 for wavelengths $\lambda < 0.55$ μm and varies little from $r_0 = 0.7$ μm to $r_0 = 0.5$ μm. In contrast, illite has ω_0 in the range from about 0.9 to 1 for $\lambda < 0.55$ μm, showing strong spectral dependence at short wavelengths. For $\lambda > 0.55$ μm, illite has ω_0 of about 0.99 for $0.55 < \lambda < 2.0$ μm and this gradually reduces to about 0.5 for $2.0 < \lambda < 5.0$ μm, while hematite shows large differences of ω_0 depending on the source of the refractive indices. The single scattering albedo decreases to about 0.35 at UV wavelengths for hematite nanoparticles (which are always observed as aggregates with other clay mineral particles) with $r_0 = 0.01$ μm and $\sigma = 2.0$, but it rapidly increases to nearly 1 at wavelengths $\lambda > 0.7$ μm.

Figure 2d compares the asymmetry parameter of hematite with refractive indices from QE1985 and LG1988 at UV and visible wavelengths with size modes of $r_0 = 0.7$, 0.5, and 0.01 μm. For $r_0 = 0.5$ and 0.7 μm, hematite from QE1985 has $g = 0.3$ - 0.99, g decreasing as λ increases. The magnitudes of g from LG1988 are in the range from 0.2 to 0.99 with a few fluctuations. For $r_0 = 0.01$ μm, both datasets put g in the range from about 0.15 to 0.38. Thus, the magnitude of g depends significantly on the particle size distribution.

3.2 Physical and mineralogical properties

3.2.1 Size and Morphology

Many electron microscopy observations (Greeland et al., 1968; Tipping, 1981; Postma and Brockenhuus-Schack, 1987; Poulton and Canfield, 2005; Raiswell and Anderson, 2005; Shi et al., 2009; Deboudt et al., 2012; Wagner et al., 2012; Guo and Barnard, 2013) have shown that poorly

ordered iron-oxides commonly occur as spheroidal to ellipsoidal nanoparticles that may be single or aggregated, and may be unattached or attached to quartz or clay minerals (Figure 3). The reasons for the aggregation and the attachment are not well understood but are likely to be related to interactions of surface charge characteristics between iron-oxides and quartz or clay minerals (Poulton and Canfield, 2005). According to Hinds (1982), the binding mechanisms that hold separate aerosols together in an agglomerate formed in the air include the van der Waals force, the electrostatic force and the surface tension of adsorbed liquid films. As mentioned above, the dispersed nanoparticles of iron-oxides which are attracted to larger dust particles have more prominent optical absorption than aggregated iron-oxides, but the use of size distributions for nanoparticles (such as r_0 = 0.01 μm and σ =2.0) will overestimate the optical absorption of iron-oxides in natural dust aerosol samples.

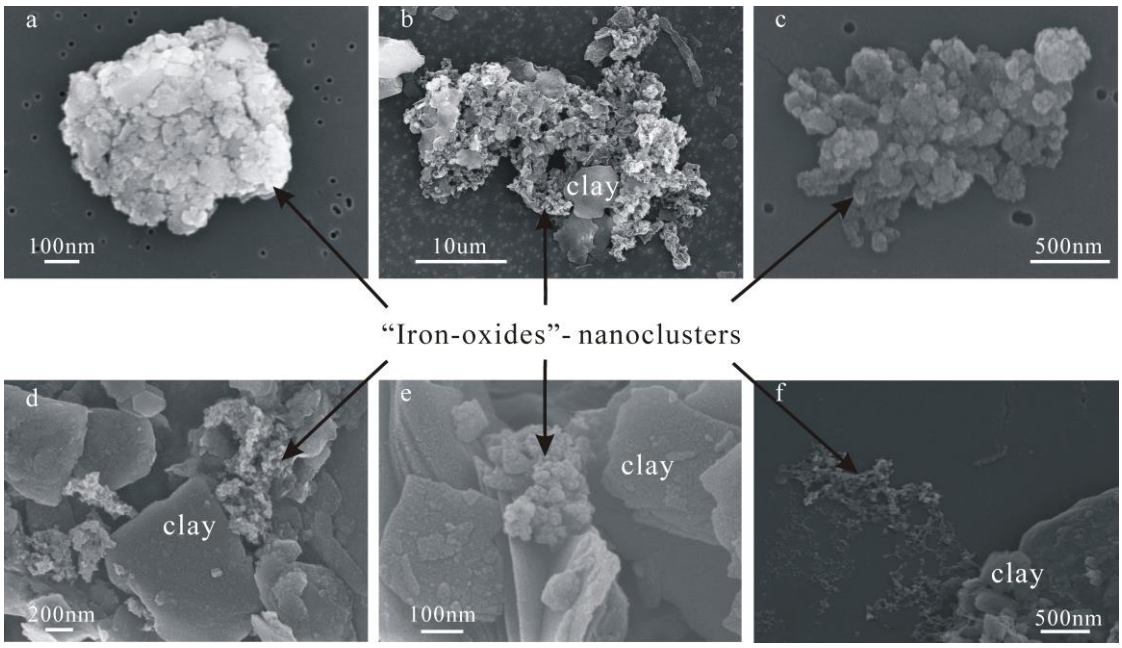

Fig. 3. Representative morphology of iron-oxide aggregates in dust samples observed by SEM.

3.2.2 Abundance of total iron and iron-oxides

By employing the optical parameters of hematite and clay minerals calculated above, we can model the optical effects of hematite in dust aerosols. Problems associated with this are the actual variation of iron-oxides content and the state of the mixture with other minerals and these should be accounted for when modeling the optical properties of dust aerosols.

The total iron content in dust aerosol bulk samples is always measured in terms of the Fe_2O_3

mass percentage of the total oxide mass by elemental analysis (i.e. XRF, PIXE or ICP). Ganor and Foner (1996) gave a median Fe content of 2.9% for dust storms in Israel. The observed Fe percentage for the Dunhuang site in China during ACE-Asia is 4.0 ± 0.9% (Zhang et al., 2003). A value of 4.45 ± 0.49% (Guieu et al., 2002) has been proposed as characterizing Saharan dust. The elemental analysis by XRF yielded total iron oxide contents between 2.0 and 5.0 weight % for four Saharan mineral dust samples of different color and origin (Linke et al., 2006b). Moreover, Lafon et al. (2004) and Lafon et al. (2006) reported that the total iron content (the Fe_2O_3 percentage) varies from 6.2% to 8.7% in six atmospheric samples and three wind tunnel generated samples. The total iron content ranges from 1.82% to 11.8% (with an especially high value of 30.0% in the sample collected from Bamako, Mali) in entrained $PM_{2.5}$ from ten soil samples representing the Arabian Peninsula, the Sahara and Sahel regions and samples from northeast Africa and south-central Asia (Moosmüller et al., 2012). Furthermore, percentage values of iron content from several datasets reported by previous studies vary mainly between 4 and 11% (e.g., Gomes and Gillette, 1993; Chiapello et al., 1997; Gao et al., 2001; Journet et al., 2014).

One additional aspect should be discussed here for the proper interpretation of the obtained data: how representative is the total iron concentration of the free iron oxide content of dust aerosols? Free-iron is present as a major aerosol component affecting the short-wavelength absorption of mineral dust. However, iron oxide represents only part of the total iron, which may also exist in the crystal lattice of numerous other dust minerals. The iron oxide-to-total iron ratio in natural and soil-derived aerosols has been characterized by applying an adapted reductive extraction method as commonly used in soil science (Lafon et al., 2004; Lafon et al., 2006). This method provides no structural information about the extractable iron and therefore cannot distinguish between the presence of goethite or hematite in the samples. Fortunately，this method can provide an upper limited to the free-iron content for the optical modeling.

Lafon et al. (2004) and Lafon et al. (2006) reported considerable variability in the iron oxide-to-total iron ratio for various regions and sampling conditions and that there is no clear relationship between the oxide-to-total iron ratio and dust origin or aging. Based on all the values for the oxide-to-total iron ratio reported in the published literature (Lafon et al., 2004; Lafon et al., 2006; Alfaro et al., 2004; Formenti et al., 2008; Klaver et al., 2011a), we have calculated an average of 0.52. Formenti et al. (2014a) reported that iron oxides account, by mass, for 0.38 to

0.72 of the total elemental iron based on X-ray absorption analysis of samples of mineral dust emitted from or transported to western Africa. Reynolds et al. (2013) reported that the percent iron in goethite and hematite relative to iron in all iron-bearing phases ranges from 0.2 to 0.52 for dust samples in Australia as determined from Mössbauer spectra. Based on an average compiled from the literature, Kandler et al. (2009) and Kandler et al. (2011) have assumed that only 20% of the total iron content is hematite when determining the complex refractive index of dust aerosols. Alfaro et al. (2004) found in their dust samples comparable total iron contents in the range of 3.0 to 6.5 weight %, and they assigned a significant amount of 2.8 to 5.8 % of this iron as present in iron oxide mineral phases. This result is consistent with the reported 2.8 - 5.0% of free-iron in aerosol samples collected from three different locations over the world (Lafon et al., 2004; Lafon et al., 2006). Takahashi et al. (2011) indicated that the content of iron-oxides is less than 5 weight % in Asian dust. Moreover, Klaver et al. (2011a) reported that the iron oxides-to-total iron ratio for the analysed samples varied between 0.4 and 0.61, accounting for between 1% and 3% of the total gravimetric mass, and Formenti et al. (2008) also illustrated that iron oxides (speciation hematite and goethite) represented 2.4% and 4.5% of the total mineral dust mass. As mentioned above, only about half of the total iron content is represented by free-iron.

XRD analytical technology has also been applied to identify the content of hematite and goethite in some cases and less than 2% iron oxides was detected (~~Bernabé et al., 2005;~~ Shi et al., 2005; Linke et al., 2006b; Kandler et al., 2009; Lawrence et al., 2010; Klaver et al., 2011a; Wagner et al., 2012; Formenti et al., 2014b). Depending on the crystal phase of interest, this method has a detection limit of 0.1 to 0.5 weight % for iron oxides (Balsam et al., 2014). Discrepancies between the quantified free-iron content detected by the method of Lafon et al. (2006) and the hematite or goethite contents determined by XRD could be due to difficulties of the Rietveld method associated with poor crystallographic ordering of iron oxides in mineral dusts.

Single particle analysis has also been conducted for detecting the free iron oxides. Fe-rich particles (iron oxides) represented no more than 5% of the particle number in aerosol samples and hematite or goethite were found more often in the fine fraction(Chou et al., 2008; Kandler et al., 2009; Schladitz et al., 2009; Kang et al., 2009; Scheuvens et al., 2011; Malek et al., 2011; Wagner et al., 2012; Menéndez et al., 2014~~; Wagner et al., 2012~~).

Table 3. Summary of global reported ratios of hematite to goethite (Hm/Gt) in dust aerosols.

Location (Number of samples)	Type	Method	Average value of Hm/Gt	Reference
Niger (1)	Aerosol*	DRS	0.5625	Lafon et al. (2006)
Tunisia (1)	Aerosol*	DRS	0.4085	Lafon et al. (2006)
China-Zhenbeitai (1)	Aerosol	DRS	0.3514	Lafon et al. (2006)
Niger (99)	Aerosol	DRS	0.4286	Formenti et al. (2008)
Niger (12)	Aerosol	XAS	0.5771	Formenti et al. (2014)
Gran Canaria (19)	Aerosol	DRS	0.9048	Lázaro et al. (2008)
North Atlantic (9)	Aerosol	DRS	0.9276	Arimoto et al. (2002)
Muztagata (7)	Aerosol	DRS	0.6918	Xu et al. (2014)+
Golmod (29)	Aerosol	DRS	0.7262	Yang et al., (2014)
Tazhong (6)	Aerosol	DRS	0.9157	Lu et al. (2011)
Dunhuang (29)	Aerosol	DRS	0.8762	Shen et al. (2006)
Yulin (32)	Aerosol	DRS	0.7158	Shen et al. (2006)
Horqin (22)	Aerosol	DRS	0.7448	Shen et al. (2006)
Australia (6)	Aerosol	MS	0.4571	Reynolds et al. (2014)

* Dust aerosol produced by wind tunnel; + Unpublished paper of the fourth author, private communication.

The technology of diffuse reflectance spectroscopy (DRS) has normally been to quantify the ratio of hematite to goethite in a particular dust sample (Lafon et al., 2006; Shen et al., 2006; Lázaro et al., 2008; Formenti et al., 2008; Formenti et al., 2014a). The accurate quantification of goethite and ferrihydrite in dust is extremely difficult owing to similarities in structure and associated absorption spectra of these two minerals (Scheinost et al., 1998; Torrent and Barrón, 2002; Schroth et al., 2009). This has the critical implication that the content of goethite measured by absorption spectroscopy is actually the sum of goethite and ferrihydrite. This does not, however, affect the optical calculations due to their optical similarity. Table 3 summarizes the measured ratios of hematite to goethite in global dust aerosol samples and shows higher ratios of Hm/Gt in Asian dust samples compared to African samples. Over the whole world, it is concluded that goethite predominates over hematite with a relative abundance of 50% - 75% of iron oxides in dust aerosols.

Based on the above reported results, we conclude that the iron-oxides account for approximately half of the mass of elemental Fe and for between 2 and 5 % of the dust mass. Most

of them are composed of goethite, representing between 50 and 75 % of the iron oxide mass.

3.2.3 Mixing states

As free-iron particles are always mixed with other kinds of particle, the condition of the mixture could be important for their ability to scatter and absorb radiation. The 3D structure of iron-oxide particles obtained by tomography reveals that these Fe-rich inclusions are often found at the surface of aluminosilicate particles but that some are also included inside particles (Deboudt et al., 2012). Inversions calculated assuming external mixing are better able to explain the wavelength dependence of dust absorption by varying only hematite concentration than inversions using internal mixing (Koven and Fung, 2006; Formenti et al., 2014a). Thus, a semi-external mixing assumption is clearly an optimal approximation for iron-oxides mixed with aluminosilicate particles. Moreover, this assumption has the advantages of simplicity of calculation, interpretation, and the possibility of comparing with model results.

3.3 Further simulation and verification

Sokolik and Toon (1999) also suggested that the radiative properties of a mixture would strongly depend on the relative abundance of individual minerals due to the large variations in the optical properties of individual minerals. Therefore, we model the optical properties for a range of possible weight fractions of hematite in the clay-size mode while the remaining mass is illite which represents the clay minerals. As mentioned above, we adopt 0% hematite as the lower limit for the aerosol samples with no free-iron particles, 2.5% hematite for the ~~advected~~ transported dust aerosol samples, 5% hematite for the locally emitted dust samples and 7.5% hematite for the upper limit. Due to the limited and discontinuous refractive indices of goethite, this setting may underestimate the actual optical effects of goethite in dust aerosol. Using the density of hematite (5.3 g/cm^3) and illite (2.75 g/cm^3), volumetric hematite fraction was converted from the mass hematite fraction to calculate the effective complex refractive indices for dust.

Dust mineralogical composition is often expressed as a weighted fraction of individual components in the total dust sample. Because the relationship of number concentration and mass concentration can be expressed as:

431 $$M_i = M_0 \cdot W_i = N_i \cdot \rho_i \cdot \frac{4}{3}\pi(r_0)^3 \cdot \exp\left[\frac{9}{2}(\ln\sigma)^2\right],$$

432 where M_i, N_i, W_i and ρ_i are the particle mass concentration, number concentration, weight
433 fraction and density of the i-th mineral in the mixture respectively and M_0 is the total particle
434 mass concentration of the mixture sample, the optical properties of external mixtures of minerals
435 can be modeled by:

436 $$K_{ext}^{mix} = \sum(K_{ext(i)}^{*} \cdot N_i) = \sum(K_{ext(i)}^{*} \cdot \frac{M_0 \cdot W_i}{\rho_i \cdot \frac{4}{3}\pi(r_0)^3 \cdot \exp\left[\frac{9}{2}(\ln\sigma)^2\right]})$$

437 Figure 4a shows the differences between the single scattering albedo calculated for the
438 mixture of illite and hematite with complex refractive indices from LG1988 at visible and infrared
439 wavelengths. Compared to ω_0 for illite with no hematite, it is not hard to see that ω_0 for mixtures
440 with different amount of hematite show significant differences in four wavelengh ranges, namely,
441 0.2 - 0.7 μm, 2.5 - 8.7 μm, 8.7 - 12.5 μm and 15.0 - 17.5 μm. For $0.2 < \lambda < 0.7$ μm and $15.0 < \lambda <$
442 17.5 μm, ω_0 for the mixtures is smaller than ω_0 for pure illite, which means the presence of
443 hematite enhances the optical absorption of the mixtures. For $2.5 < \lambda < 8.7$ μm, ω_0 for the
444 mixtures is larger than for pure illite, which means the presence of hematite enhances the optical
445 scattering of the mixtures. But for $8.7 < \lambda < 12.5$ μm, ω_0 shows more complicated fluctuations.
446

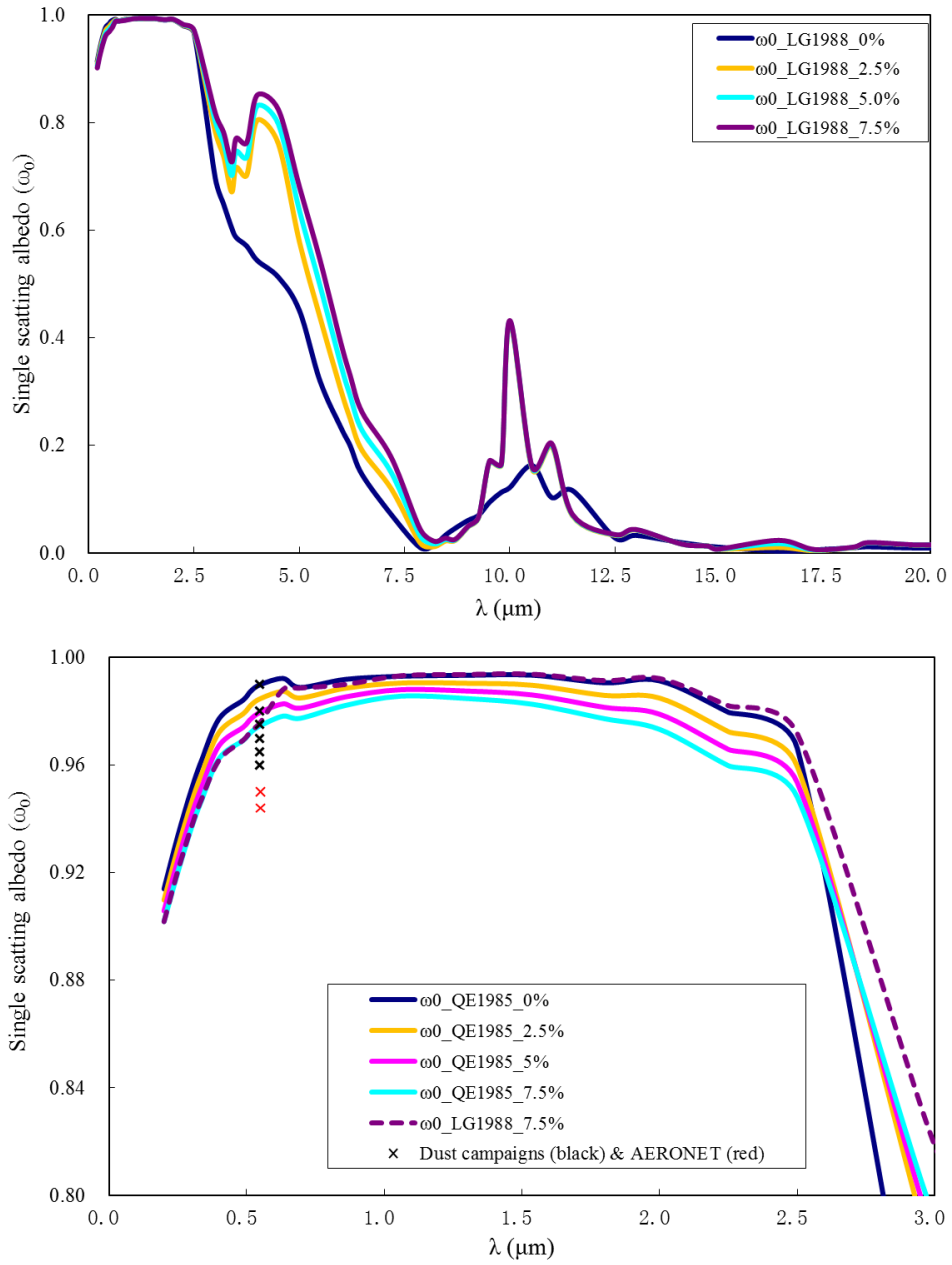

Fig. 4. Spectral single scatting albedo (SSA) for mixtures of illite and hematite with varying percentages and refractive indices at wavelengths of 0-20 μm (a) and 0-3 μm (b) with comparison to field observed results at 550nm..

Figure 4b shows the differences between ω_0 for illite mixed with different amounts of hematite with refractive indices from QE1985 at solar wavelengths. The magnitude of ω_0 for a mixture increases when the median radius r_0 increases. In order to compare the effects for hematite with refractive indices from two different sources for the same mixture state, we also plot ω_0 for illite mixed with 7.5% hematite with refractive indices from LG1988 in Figure 4b.

457 Evidently, for $0.55 < \lambda < 2.5$ μm, the dataset of QE1985 will lead to higher optical absorption,
458 although the two datasets have the same optical scattering and absorption for $\lambda < 0.55$ μm.

459 Another coming question is what is the competition between theoretical calculated values
460 and field observed results? In order to compare our calculated SSAs with measured values, we
461 review all reported SSAs during different dust campaigns or inferred from AERONET
462 measurements, and listed them in Table 4. The measured results for dust mixed with BC were
463 excluded during our review progress, such as the results from the campaign of AMMA. The
464 measurements from DABEX are comparable but on the lower edge of previous measurements
465 performed at 550 nm during the TARFOX, SHADE, GERBILS, SAMUM, NAMMA and Fennec
466 2011 field campaigns. Absorption from the mineral dust as measured using the corrected
467 nephelometer and Particle Soot Absorption Photometer (PSAP) combination suggests that single
468 scattering albedos at 550 nm (SSA550) range from 0.91 to 0.97 (with a mean of 0.97) for iron
469 oxide mass fractions between 1.3 and 3.5% (Klaver et al., 2011a). The SSAs at 532 nm were
470 reported as 0.99 ±0.001 and 0.98 ± 0.002 for the Cairo 2 and Morocco dust samples with Fe_2O_3
471 mass fractions of 4.5 and 3.63%, respectively (Linke et al., 2006). Johnson and Osborne (2011)
472 revealed that the use of the mineral dust refractive indices from Balkanski et al. (2007) assuming
473 1.5% hematite gave reasonable agreement with the measured single scattering albedo, consistent
474 with the findings of Klaver et al. (2011a). Haywood et al. (2011) shown that mineral dust is
475 relatively non-absorbing at 550 nm due to the relatively small fraction of iron oxides present (1–
476 3%). Balkanski et al. (2007) addressed this difference and argued that dust absorption at visible
477 wavelengths might be lower than previously thought because mixing rule calculations with
478 hematite content of 1.5% by volume, supposedly representative of median dust absorption,
479 showed a very good agreement with the AERONET measurements. The same question is
480 presented in Figure 7a of Formenti et al. (2014a): that the calculated SSA using a higher
481 imaginary index of iron-oxides also overestimated the absorbing ability of Saharan dust in
482 comparison with field observation.

483 We compare our calculated SSA curves with the measured values in Figure 4b. It is shown
484 that the observed SSAs were mostly ranged in 0.94-0.99 during different dust campaigns, but
485 much lower (0.944-0.95) for the AERONET which cannot exclude the presence of black carbon
486 with higher absorbing. Our calculated result could consistent with the higher part (0.97-0.99) of

measured SSAs, but higher than the lower part (0.95-0.97) due to the effect of coarse particles during different dust campaigns. Thus, the iron oxide content alone cannot explain the variability of the single scattering albedo. This suggests that more complete knowledge of the dust mineralogical composition and size distribution with varied multi-modes is needed as input to more rigorous modeling.

Table 4. Review of measured dust single scattering albedos during dust campaigns and AERONET observations.

References	SSA_550nm (Mean)	S.D.	Observations
Haywood et al. (2001)	0.97	0.02	TARFOX
Haywood et al. (2003)	0.97	0.02	SHADE
Johnson and Osborne (2011)	0.97	0.02	GERBILS
Müller et al. (2011)	0.96	0.03	SAMUM_2
Petzold et al. (2011)	0.975	0.15	SAMUM
Jeong et al. (2008)	0.96	0.01	NAMMA
Osborne et al. (2008)	0.99	0.02	DABEX
Ryder et al. (2013)	0.965	0.015	Fennec 2011
Lack et al. (2009)	0.95	0.01	TexAQS/GoMACCS
Linke et al. (2006)	0.985	0.006	Laboratory
Zhu et al. (2007)	0.95	0.01	AERONET
Kim et al. (2011)	0.944	0.005	AERONET

In order to check the further effects of the mixing state of hematite on the single scattering albedo, we use two sets of assumptions that bracket the actual state of hematite mixing: internal mixing (Int), in which individual dust particles are a combination of all components present; and external mixing (Ext), in which different components exist as separate particles.

For the case of an external mixture of particles, the average optical properties are calculated by summing over the optical properties of the individual species. Approximations have to be made to calculate the optical properties of internal mixed particles. Three common approximations for the calculation of these latter optical properties are the volume mixing method, the Bruggeman approximation and the Maxwell-Garnett approximation (Chýlek et al., 1988; Bohren and Huffman, 1998). Detail information about the three methods is given by Sokolik and Toon (1999). We have calculated the single scattering albedo (SSA) of illite-hematite mixtures with different hematite contents using internal mixing according to the above three internal approximations and also using external mixing.

The calculated SSA values for illite-hematite mixtures using internal and external mixture

assumptions as a function of wavelength and hematite mass fraction are illustrated in Figure 5. For the case of external mixing, the SSAs at 405 nm show good agreement for refractive indices from QE1985 and LG1988, but the calculated SSAs at 870 nm for hematite with refractive indices from QE1985 are much smaller than those using LG1988. This is explained by Figure 4b where the two datasets have the same optical scattering and absorbing properties for $\lambda < 0.55$ μm but the dataset of QE1985 leads to higher optical absorption for $\lambda > 0.55$ μm. The calculated SSAs with the three different internal mixing methods are all much smaller than those for external mixing both at 405 nm and 870 nm since the assumption of an external mixture results in less absorption and less wavelength dependence of absorption than does the assumption of an internal mixture for small amounts of hematite. The basic reason for this is due to the extremely high imaginary refractive index for hematite at short wavelengths. For the case of internal mixing, the SSAs from the volume mixing method are smaller than for the other methods. This is due to the averaged imaginary refractive index being larger than for the other two approximations. On the basis of the study of Peterson (1968), only the effective refractive index of the non-metallic part of the dust can be calculated using the volume mixing method. Thus, adopting the volume mixing method to calculate the optical properties of aerosol samples will lead to a smaller SSA (Levoni et al., 1997; Sokolik and Toon, 1999; Shi et al., 2005; Höller et al., 2003; Ebert et al., 2004; Kandler et al., 2007; Kandler et al., 2009; Petzold et al., 2009; Otto et al., 2009; Wagner et al., 2012).

The calculated SSAs using the Bruggeman approximation are consistent with those from the Maxwell-Garnet approximation for low hematite contents at both 405 nm and 870 nm but differ from them for hematite content larger than 10%. Both the Maxwell-Garnet and Bruggeman approximations are derived from the same integral equation for the propagation of electromagnetic waves in an inhomogeneous medium but under a different set of approximations (Chyýlek et al., 1988; Bohren and Huffman, 1998). In previous studies, the Bruggeman approximation (Sokolik and Toon, 1999; Lafon et al., 2006; Koven and Fung, 2006; Mishra and Tripathi, 2008; Thomas and Gautier, 2009; McConnell et al., 2010; Klaver et al., 2011a; Wagner et al., 2012; Mishra et al., 2012~~; Thomas and Gautier, 2009~~) has been more often used for calculating the complex refractive index of silicate-hematite mixtures than the Maxwell-Garnet approximations (Balkanski et al., 2007; Hansell Jr et al., 2011).

The Bruggeman approximation allows for the calculation of an effective dielectric constant

of multicomponent mixtures without distinguishing between matrix and inclusions. If we do not know which is the main body for the silicate and the hematite in an aerosol, it is better to choose the Bruggeman approximation. For the Maxwell-Garnet approximation a decision must be made as to which component is the matrix and which is an inclusion. The Maxwell-Garnett approximation is designed for small inclusions inside a host matrix and thus it is not suitable for hematite >50% in the mixture, so the calculated SSAs show abnormal fluctuation for hematite >50% in Figure 5. This phenomenon disappears if we consider the inverse Maxwell-Garnet approximation which makes hematite the host matrix. Actually, the variation of Fe_2O_3 has been constrained within the range 0–10%, so we advise the use of the Maxwell-Garnet approximation in which the inclusions should be identical in composition but may be different in volume, shape and orientation.

The comparison between the laboratories measured SSAs with known abundance of iron-oxides with our theoretically calculated SSAs by different mixing rules, would give us further insights into the actual mixing states of iron oxides and accuracy of different refractive indices. Laboratory measured SSAs ~~for entrained soil samples with known abundance of iron oxides~~ by extinction and photoacoustic absorption measurements at different wavelengths have been reported in Linke et al. (2006a) and Moosmüller et al. (2012). Moosmüller et al (2012) has demonstrated ~~The latter shows~~ that SSAs are much smaller at 405 nm than at 870 nm and that SSAs at both wavelengths are dominated by and linearly correlated with the iron content ~~of the entrained mineral dust~~. These measured results are also shown in Figure 5 for comparison with our theoretically calculated SSAs. The measured SSAs at 405 nm show good agreement with our external mixing SSA values calculated from both LG1988 and QE1985 for hematite less than ~~<~~10% , while they are much larger than our internal mixing SSA values at ~~this wavelength~~ 405 nm (Figure 5a), potentially indicating that ~~their~~ the dust samples are mainly external mixing and are accompanied by ~~with~~ a very small degree of internal mixing.

In contrast, ~~their~~ the measured SSA values at 870 nm are much larger than our external and internal mixing SSA values calculated from refractive indices from QE1985 but show good agreement with our external mixing SSA values calculated using LG1988 values (Figure 5b). This illustrates the fact that the complex refractive indices of hematite from QE1985 have greatly overestimated absorption at 870 nm.

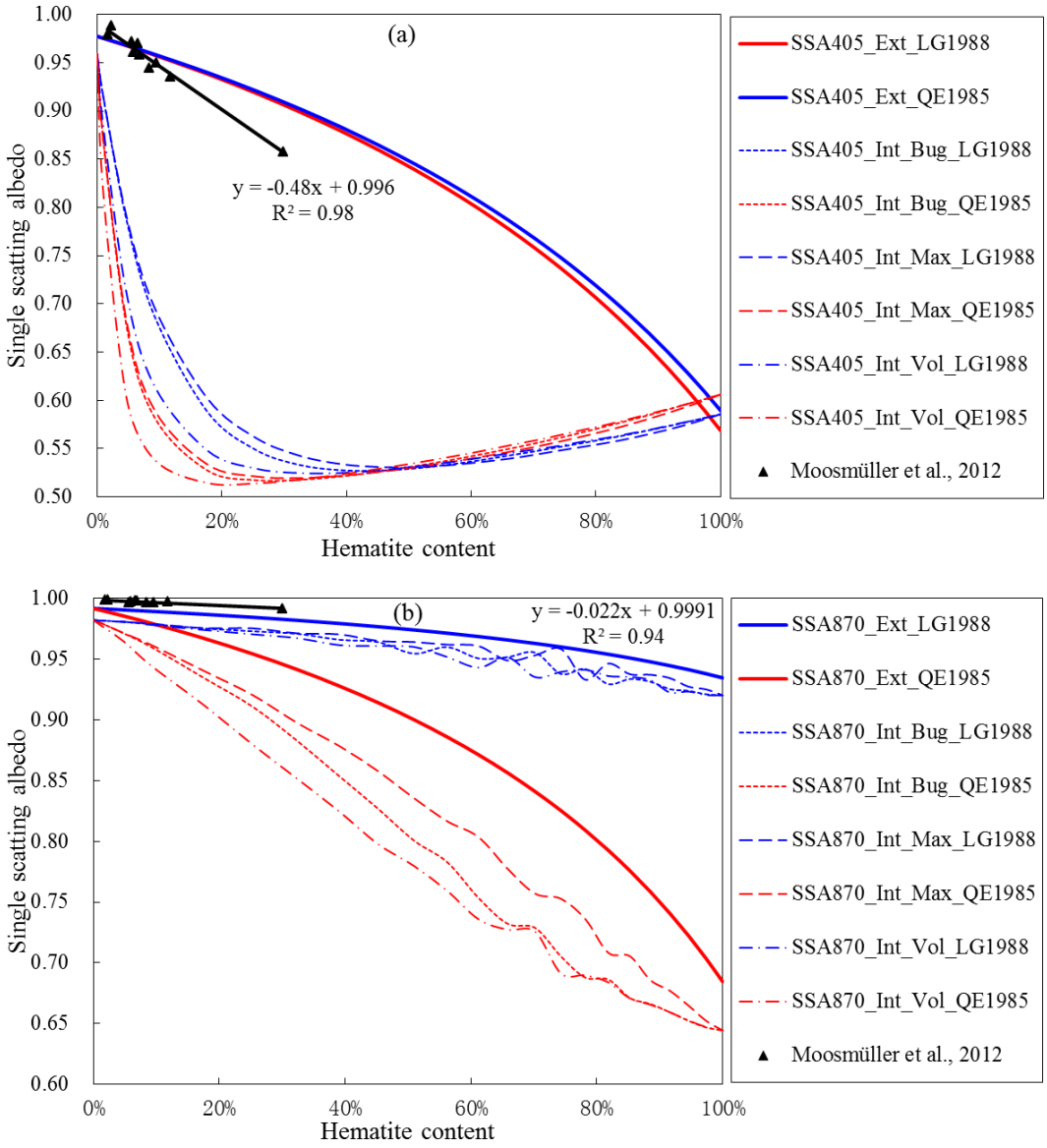

Fig. 5. The single scattering albedo (SSA) as a function of varying hematite content at wavelengths of (a) 405 and (b) 870 nm, with different mixing states (Internal and External mixing), different complex refractive index sources (QE1985 and LG1988) and mixing approximations (Volume, Maxwell-Garnet and Bruggeman). For comparison, the measured values using a photoacoustic instrument with integrating reciprocal nephelometer and linear fits from Moosmüller et al.(2012) are also shown.

For purposes of quantitatively illustrating the optical effects of hematite in the mixtures, we calculate $\Delta\omega_0$ as the difference between the single scattering albedo of ~~a~~ mixtures with given abundances of hematite and pure illite ~~mixture and the single scattering albedo of pure illite. The latter represents the case when the dust contains no hematite~~. Thus, we have

$$\Delta\omega_0 = \frac{\omega_0^{mixture} - \omega_0^{illite}}{\omega_0^{illite}} \times 100\%.$$

Here, we assume $M_0 = 100$ μg/cm^3 and a lognormal size distribution with r_0 = 0.5 μm, σ = 2.0. The single scattering albedo of pure illite represents the case when the dust contains no hematite. If the calculated values of $\Delta\omega_0$ are negative, this means that hematite has high absorption at the corresponding wavelengths. Figure 6 shows $\Delta\omega_0$ calculated for hematite with refractive indices from QE1985 and LG1988 at ~~wavelengths less than~~ λ < 20 μm. ~~We assume $M_0 = 100$ μg/cm^3 and a lognormal size distribution with r_0 = 0.5 μm, σ = 2.0. If the values of $\Delta\omega_0$ are negative, this means that hematite has high absorption at the corresponding wavelengths.~~ ~~Figure 6~~ It demonstrates that hematite with refractive indices from LG1988 only enhances the optical absorption of ~~aerosol~~ dust mixtures for λ < 0.55 μm, but hematite with refractive indices from QE1985 enhances the absorption for λ < 2.5 μm ~~from UV to visible wavelengths~~. The magnitude of $\Delta\omega_0$ for 5% hematite over these wavelength is approximately about 1%. Therefore, the use of refractive indices for hematite from QE1985 in climate models would lead to overestimation of the optical absorption at both visible and near-IR wavelengths. Another apparent difference is the positive magnitude of $\Delta\omega_0$ for hematite with refractive indices from the two datasets at wavelengths of 2.5 < λ < 8.7 μm. ~~Therefore, the employment of refractive indices for hematite from QE1985 in climate models would lead to overestimation of the optical absorption at both visible and near-IR wavelengths.~~

~~Absorption from the mineral dust as measured using the corrected nephelometer and Particle Soot Absorption Photometer (PSAP) combination suggests that single scattering albedos at 550 nm (SSA550) range from 0.91 to 0.97 (with a mean of 0.97) for iron oxide mass fractions between 1.3 and 3.5% (Köhler et al., 2011). The SSAs at 532 nm were reported as 0.99±0.001 with Fe_2O_3 mass fraction of 4.5% for Cairo 2 and 0.98 ± 0.002 with Fe_2O_3 mass fraction of 4.5% for Morocco (Linke et al., 2006a). Johnson and Osborne (2011) revealed that the use of the mineral dust refractive indices from Balkanski et al. (2007) assuming 1.5% hematite gave reasonable agreement with the measured single scattering albedo, consistent with the findings of Klaver et al. (2011a). Haywood et al. (2011) shown that mineral dust is relatively non-absorbing at 550 nm due to the relatively small fraction of iron oxides present (1–3%).~~

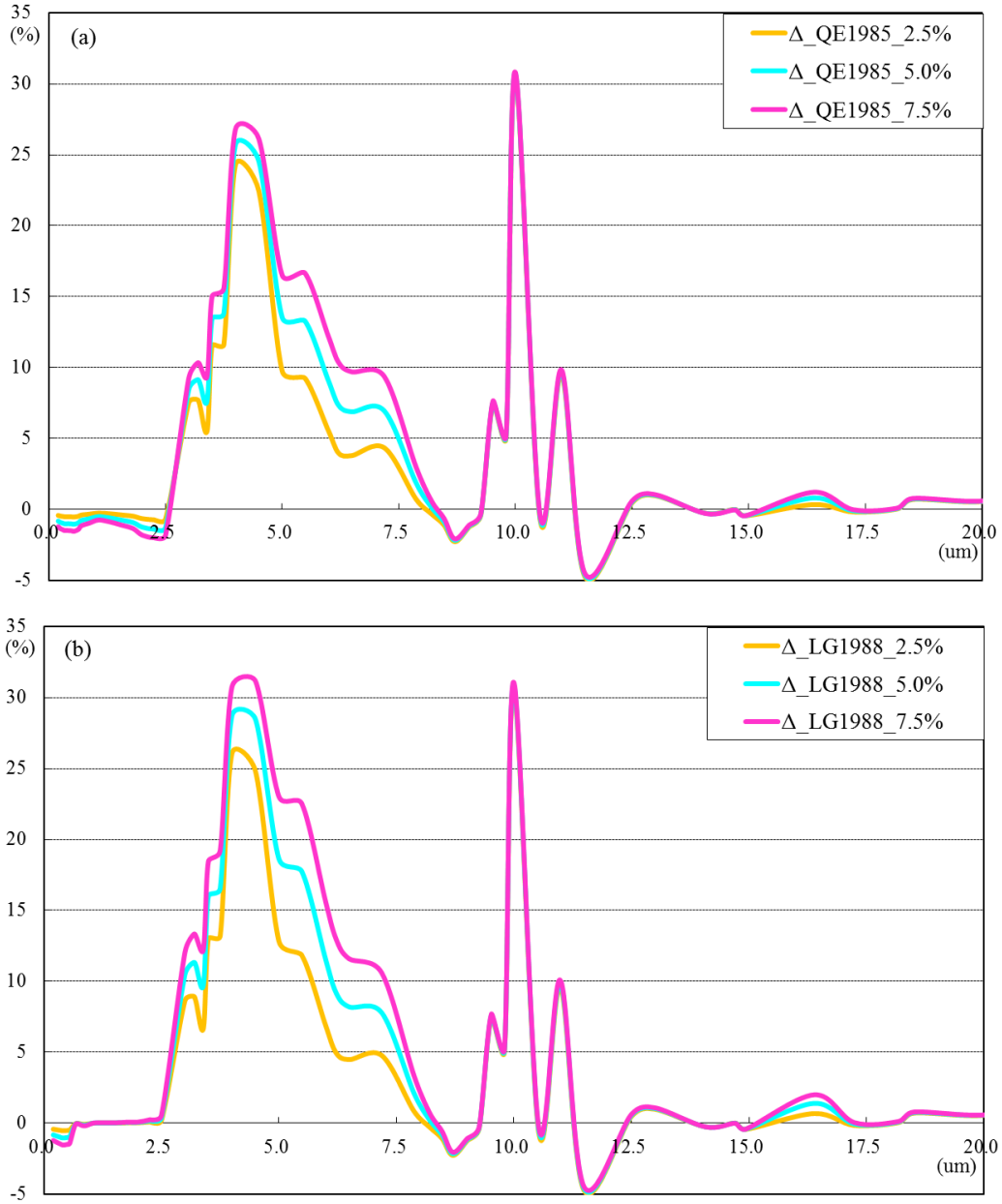

Fig. 6. The difference $\Delta\omega_0$ between the single scattering albedo (SSA) of pure illite and the single scattering albedo of mixtures with different contents and refractive indices of hematite. (a) Complex refractive index of hematite from Qurrey (1985), (b) Complex refractive index of hematite from Longtin (1988).

~~Balkanski et al. (2007) addressed this difference and argued that dust absorption at visible wavelengths might be lower than previously thought because mixing rule calculations with a hematite content of 1.5 volume %, supposed to be representative for median dust absorption, showed a very good agreement with the AERONET measurements. The same question is presented in Figure 7a of (Formenti et al., 2014): that the calculated SSA using a higher imaginary index of iron oxides also overestimated the absorbing ability of Saharan dust in comparison with~~

~~field observation.~~

Given all that, the complex refractive index of iron-oxides is therefore a key parameter in effects of dust aerosols on the radiation balance, and the optical constants of hematite from different sources become a major source of uncertainty in radiative forcing calculation. Further work is needed to provide experimental measurements of the refractive index of iron-oxides, especially for hematite and goethite in the visible region of the spectrum. More complete knowledge of the dust mineralogy, morphology and size distribution with varied multi-modes is needed as input to more rigorous modeling.

4. Summary

In this paper we have investigated the spectral optical properties of iron-oxides with considering different refractive indices, size distributions, and more logical weight fractions and mixing states of iron-oxides. The iron-oxides account for approximately half of the mass of elemental Fe and for between 2 and 5 % of the dust mass. Most of them are composed of goethite, representing between 50 and 75 % of the iron oxide mass. The iron-oxides commonly occur as spheroidal to ellipsoidal nanoparticles that may be single or aggregated, and may be unattached or attached to quartz or clay minerals, which could be expressed as semi-external mixing state. Moreover, the spectral SSA values determined in the present study show a strong wavelength-dependence with a steep decrease from the visible to the near-UV. There are still problems that need to be solved in order to accurately study the real role of iron-oxides in determining the overall impact of dust aerosols on climate ~~forcing~~petrubation, as follows:

1. Although there have been many published investigations of the complex refractive index of different iron-oxides, uniformly continuous optical constants for a single type of iron-oxides from 0.2 um to 50 μm are very scarce. Some of them are inconsistent and careful checking of their accuracy is therefore essential.

2. The abundance of specific iron-oxide types (such as goethite and magnetite) remains unknown. Although many studies have measured the mass ratio of goethite to hematite as about 7:3, the absence of goethite optical constants at 0.75-8.5 μm restricts the usefulness of this ratio. Thus, using hematite to represent all types of iron-oxides is a popular hypothesis.

3. Microscopic observations and optical simulations have shown that semi-external mixtures

employing both external mixtures of Fe-aggregates and other minerals and partly internal mixing between iron-oxides and aluminosilicate particles is the optimal mixing approximation.

4. For hematite, there are two datasets of complex refractive indices that differ significantly. Compared with LG1988, the complex refractive indices of QE1985 greatly overestimate the optical absorption at both visible and near-IR wavelengths. Comprehensive laboratory measurements of the refractive indices of iron-oxides, especially of hematite and goethite in the visible spectrum, should therefore be made in order to accurately assess the effect of mineral dust on climate perturbation.

Theoretically calculated SSA values are comparable to values observed in recent laboratory and field studies in the range of 0.97-0.99. The iron oxide content alone cannot explain the variability of the single scattering albedo, and the lower SSAs could be explained as the presence of coarse dust particles and high-absorbing black carbon in natural transported dust aerosol. More complete knowledge of the dust mineralogical composition and size distribution with dynamic varied multi-modes is needed as input to more rigorous modeling.

~~As about 87% of solar spectral irradiance is distributed at wavelengths from 0.4 μm to 2.5 μm (ASTM-G-173, http://rredc.nrel.gov/solar/spectra/am1.5/), hematite with refractive indices from LG1988 shows approximately equal absorption to the clay mineral illite over the whole region from 0.2 μm to 2.5 μm, and only enhances the optical absorption of aerosol mixtures at $\lambda < 0.55$ μm. Thus, a more precise description of the nature of clays and iron oxides is necessary at lower wavelengths because of large differences in their spectral optical properties. Comprehensive laboratory measurements of the refractive indices of iron-oxides, especially of hematite and goethite in the visible spectrum, should therefore be made in order to accurately assess the effect of mineral dust on climate forcing.~~

Acknowledgement

We are grateful to Dr. Yahui Yue at ITPCAS and Dr. Yongliang Li at BNU for completing the SEM–EDX analysis and Dr. Michael Mishchenko at NASA GISS for offering the T-matrix and Lorenz-Mie codes. This work was supported by the National Natural Science Foundation of China (Grant No. 41205108 and 41271074).

678

679 **References**

680 Alfaro, S., Lafon, S., Rajot, J., Formenti, P., Gaudichet, A., and Maille, M.: Iron oxides and light
681 absorption by pure desert dust: An experimental study, Journal of Geophysical Research:
682 Atmospheres (1984–2012), 109, 2004.
683 Anderson, B., and Jenne, E.: Free-iron and-manganese oxide content of reference clays, Soil Science,
684 109, 163-169, 1970.
685 ~~Angel, B., and Vincent, W.: Associated with the surface of kaolins, Clays and Clay Minerals, 26,~~
686 ~~263-272, 1978.~~
687 Arimoto R., Balsam W., and Schloesslin C.: Visible spectroscopy of aerosol particles collected on
688 filters: iron-oxide minerals. Atmospheric Environment, 36(1), 89-96, 2002.
689 Arimoto, R., Ray, B., Lewis, N., Tomza, U., and Duce, R.: Mass‐particle size distributions of
690 atmospheric dust and the dry deposition of dust to the remote ocean, Journal of Geophysical
691 Research: Atmospheres (1984–2012), 102, 15867-15874, 1997.
692 Balkanski, Y., Schulz, M., Claquin, T., and Guibert, S.: Reevaluation of Mineral aerosol radiative
693 forcings suggests a better agreement with satellite and AERONET data, Atmospheric Chemistry and
694 Physics, 7, 81-95, 2007.
695 Balsam, W., Ji, J., Renock, D., Deaton, B. C., and Williams, E.: Determining hematite content from
696 NUV/Vis/NIR spectra: Limits of detection, American Mineralogist, 99, 2280-2291, 2014.
697 Baltrusaitis, J., Cwiertny, D. M., and Grassian, V. H.: Adsorption of sulfur dioxide on hematite and
698 goethite particle surfaces, Physical Chemistry Chemical Physics, 9, 5542-5554, 2007.
699 Bedidi, A., and Cervelle, B.: Light scattering by spherical particles with hematite and goethitelike
700 optical properties: Effect of water impregnation, Journal of Geophysical Research: Solid Earth
701 (1978–2012), 98, 11941-11952, 1993.
702 ~~Bernabé, J., Carretero, M., and Galán, E.: Mineralogy and origin of atmospheric particles in the~~
703 ~~industrial area of Huelva (SW Spain), Atmospheric Environment, 39, 6777-6789, 2005.~~
704 Bohren, C. F., and Huffman, D. R.: Absorption and scattering of light by small particles, John Wiley &
705 Sons, 1998.
706 Claquin, T., Schulz, M., Balkanski, Y. J.: Modeling the mineralogy of atmospheric dust sources, J.
707 Geophys. Res. -Atmos., 104(D18), 22243-22256, doi:10.1029/1999JD900416, 1999.
708 Chiapello, I., Bergametti, G., Chatenet, B., Bousquet, P., Dulac, F., and Soares, E. S.: Origins of
709 African dust transported over the northeastern tropical Atlantic, Journal of Geophysical Research:
710 Atmospheres (1984–2012), 102, 13701-13709, 1997.
711 Chou, C., Formenti, P., Maille, M., Ausset, P., Helas, G., Harrison, M., and Osborne, S.: Size
712 distribution, shape, and composition of mineral dust aerosols collected during the African Monsoon
713 Multidisciplinary Analysis Special Observation Period 0: Dust and Biomass‐Burning Experiment
714 field campaign in Niger, January 2006, Journal of Geophysical Research: Atmospheres (1984–
715 2012), 113, 2008.
716 Chýlek, P., Srivastava, V., Pinnick, R. G., and Wang, R.: Scattering of electromagnetic waves by
717 composite spherical particles: experiment and effective medium approximations, Applied Optics, 27,
718 2396-2404, 1988.
719 Cornell, R. M., and Schwertmann, U.: The iron oxides: structure, properties, reactions, occurrences and
720 uses, John Wiley & Sons, 2006.

Dang, C., and Hegg, D. A.: Quantifying light absorption by organic carbon in western North American snow by serial chemical extractions, Journal of Geophysical Research: Atmospheres, 119, 10,247-210,261, 2014.

Dave, J., and Center, I. P. A. S.: Subroutines for computing the parameters of the electromagnetic radiation scattered by a sphere, IBM Scientific Center, 1968.

Deboudt, K., Gloter, A., Mussi, A., and Flament, P.: Red‐ox speciation and mixing state of iron in individual African dust particles, Journal of Geophysical Research: Atmospheres (1984–2012), 117, 2012.

Derimian, Y., Karnieli, A., Kaufman, Y., Andreae, M., Andreae, T., Dubovik, O., Maenhaut, W., and Koren, I.: The role of iron and black carbon in aerosol light absorption, Atmospheric Chemistry and Physics, 8, 3623-3637, 2008.

Dupart, Y., King, S. M., Nekat, B., Nowak, A., Wiedensohler, A., Herrmann, H., David, G., Thomas, B., Miffre, A., and Rairoux, P.: Mineral dust photochemistry induces nucleation events in the presence of SO2, Proceedings of the National Academy of Sciences, 109, 20842-20847, 2012.

Ebert, M., Weinbruch, S., Hoffmann, P., and Ortner, H. M.: The chemical composition and complex refractive index of rural and urban influenced aerosols determined by individual particle analysis, Atmospheric Environment, 38, 6531-6545, 2004.

Formenti, P., Rajot, J. L., Desboeufs, K., Caquineau, S., Chevaillier, S., Nava, S., Gaudichet, A., Journet, E., Triquet, S., and Alfaro, S.: Regional variability of the composition of mineral dust from western Africa: Results from the AMMA SOP0/DABEX and DODO field campaigns, Journal of Geophysical Research: Atmospheres (1984–2012), 113, 2008.

Formenti, P., Schütz, L., Balkanski, Y., Desboeufs, K., Ebert, M., Kandler, K., Petzold, A., Scheuvens, D., Weinbruch, S., and Zhang, D.: Recent progress in understanding physical and chemical properties of African and Asian mineral dust, Atmospheric Chemistry and Physics, 11, 8231-8256, 2011.

Formenti, P., Caquineau, S., Chevaillier, S., Klaver, A., Desboeufs, K., Rajot, J., Belin, S., and Briois, V.: Dominance of goethite over hematite in iron oxides of mineral dust from Western Africa: Quantitative partitioning by X-ray absorption spectroscopy, Journal of Geophysical Research: Atmospheres, 2014a.

Formenti, P., Caquineau, S., Desboeufs, K., Klaver, A., Chevaillier, S., Journet, E., and Rajot, J.: Mapping the physic-chemical properties of mineral dust in western Africa: mineralogical composition, Atmos. Chem. Phys., 14, 10663–10686, doi:10.5194/acp-14-10663-2014, 2014b.

Galuza, A., Eremenko, V., and Kirichenko, A.: Analysis of hematite reflection spectrum by the Kramers-Kronig method, Sov. Phys. Solid State, 21, 654-656, 1979.

Ganor, E., and Foner, H.: The mineralogical and chemical properties and the behaviour of aeolian Saharan dust over Israel, in: The impact of desert dust across the Mediterranean, Springer, 163-172, 1996.

Gao, Y., Kaufman, Y., Tanre, D., Kolber, D., and Falkowski, P.: Seasonal distributions of aeolian iron fluxes to the global ocean, Geophysical Research Letters, 28, 29-32, 2001.

Gillespie, J. B., and Lindberg, J. D.: Ultraviolet and visible imaginary refractive index of strongly absorbing atmospheric particulate matter, Applied optics, 31, 2112-2115, 1992.

Ginot, P., Dumont, M., Lim, S., Patris, N., Taupin, J.-D., Wagnon, P., Gilbert, A., Arnaud, Y., Marinoni, A., and Bonasoni, P.: A 10 year record of black carbon and dust from a Mera Peak ice core (Nepal): variability and potential impact on melting of Himalayan glaciers, The Cryosphere, 8, 1479-1496,

765 2014.
766 Glotch, T. D., and Rogers, A. D.: Evidence for aqueous deposition of hematite - and sulfate - rich
767 light - toned layered deposits in Aureum and Iani Chaos, Mars, Journal of Geophysical Research:
768 Planets (1991 – 2012), 112, 2007.
769 Glotch, T. D., and Rossman, G. R.: Mid-infrared reflectance spectra and optical constants of six iron
770 oxide/oxyhydroxide phases, Icarus, 204, 663-671, 2009.
771 Gomes, L., and Gillette, D. A.: A comparison of characteristics of aerosol from dust storms in central
772 Asia with soil-derived dust from other regions, Atmospheric Environment. Part A. General Topics,
773 27, 2539-2544, 1993.
774 Greenland, D. J., Oades, J., and Sherwin, T.: Elecrron-microscope observations of iron oxides in some
775 red soils, Journal of Soil Science, 19, 123-126, 1968.
776 Guieu, C., Loÿ - Pilot, M. D., Ridame, C., and Thomas, C.: Chemical characterization of the Saharan
777 dust end - member: Some biogeochemical implications for the western Mediterranean Sea, Journal
778 of Geophysical Research: Atmospheres (1984 – 2012), 107, ACH 5-1-ACH 5-11, 2002.
779 Guo, H., and Barnard, A. S.: Naturally occurring iron oxide nanoparticles: morphology, surface
780 chemistry and environmental stability, Journal of Materials Chemistry A, 1, 27-42, 2013.
781 Höller, R., Ito, K., Tohno, S., and Kasahara, M.: Wavelength - dependent aerosol single - scattering
782 albedo: Measurements and model calculations for a coastal site near the Sea of Japan during ACE -
783 Asia, Journal of Geophysical Research: Atmospheres (1984 – 2012), 108, 2003.
784 Hansell Jr, R., Reid, J., Tsay, S., Roush, T., and Kalashnikova, O.: A sensitivity study on the effects of
785 particle chemistry, asphericity and size on the mass extinction efficiency of mineral dust in the
786 earth's atmosphere: from the near to thermal IR, Atmospheric chemistry and Physics, 11, 1527-1547,
787 2011.
788 Haywood, J., Francis, P., Glew M., and Taylor, J.: Optical properties and direct radiative effect of
789 Saharan dust: A case study of two Saharan dust outbreaks using aircraft data, J. Geophys.
790 Res.-Atmos., 106(D16), 18417-18430, doi:10.1029/2000JD900319, 2001.
791 Haywood, J., Francis, P., Osborne, S., Glew, M., Loeb, N., Highwood, E., Tanré, D., Myhre, G.,
792 Formenti, P., and Hirst, E.: Radiative properties and direct radiative effect of Saharan dust measured
793 by the C-130 aircraft during SHADE: 1. Solar spectrum, J. Geophys. Res.-Atmos., 108(D18), 8577,
794 doi:10.1029/2002JD002687, 2003.
795 Haywood, J., Johnson, B., Osborne, S., Baran, A., Brooks, M., Milton, S., Mulcahy, J., Walters, D.,
796 Allan, R., and Klaver, A.: Motivation, rationale and key results from the GERBILS Saharan dust
797 measurement campaign, Quarterly Journal of the Royal Meteorological Society, 137, 1106-1116,
798 2011.
799 Henning, T., Begemann, B., Mutschke. H.. and Dorschner, J.: Optical properties of oxide dust
800 grains. Astron. Astrophys. Suppl. Ser., 112, 143-149, 1995.
801 Henning T. and Mutschke H.: Low-temperature infrared properties of cosmic dust analogues. Astron.
802 Astrophys., 327, 743-754, 1997.
803 Hinds, W. C.: Aerosol technology: properties, behavior, and measurement of airborne particles, New
804 York, Wiley-Interscience, 1982. 442 p., 1, 1982.
805 Hsu, W. P., and Matijević, E.: Optical properties of monodispersed hematite hydrosols, Applied optics,
806 24, 1623-1630, 1985.
807 Jeong, M. J., Tsay, S. C., Ji, Q., Hsu, N. C., Hansell, R. A., and Lee, J.: Ground-based measurements of
808 airborne Saharan dust in marine environment during the NAMMA field experiment, Geophys. Res.

Lett., 35, L20805, doi:10.1029/2008GL035587,2008.
Jickells, T., An, Z., Andersen, K. K., Baker, A., Bergametti, G., Brooks, N., Cao, J., Boyd, P., Duce, R., and Hunter, K.: Global iron connections between desert dust, ocean biogeochemistry, and climate, science, 308, 67-71, 2005.
Johnson, B., and Osborne, S.: Physical and optical properties of mineral dust aerosol measured by aircraft during the GERBILS campaign, Quarterly Journal of the Royal Meteorological Society, 137, 1117-1130, 2011.
Journet, E., Balkanski, Y., and Harrison, S.: A new data set of soil mineralogy for dust-cycle modeling, Atmospheric Chemistry and Physics, 14, 3801-3816, 2014.
Kandler, K., Benker, N., Bundke, U., Cuevas, E., Ebert, M., Knippertz, P., Rodr ́guez, S., Sch ̈utz, L., and Weinbruch, S.: Chemical composition and complex refractive index of Saharan Mineral Dust at Izana, Tenerife (Spain) derived by electron microscopy, Atmospheric Environment, 41, 8058-8074, 2007.
Kandler, K., Sch ̈utz, L., Deutscher, C., Ebert, M., Hofmann, H., J ̈ackel, S., Jaenicke, R., Knippertz, P., Lieke, K., and Massling, A.: Size distribution, mass concentration, chemical and mineralogical composition and derived optical parameters of the boundary layer aerosol at Tinfou, Morocco, during SAMUM 2006, Tellus B, 61, 32-50, 2009.
Kandler, K., Lieke, K., Benker, N., Emmel, C., Küpper, M., MÜLLER - EBERT, D., Ebert, M., Scheuvens, D., Schladitz, A., and Sch ̈utz, L.: Electron microscopy of particles collected at Praia, Cape Verde, during the Saharan Mineral Dust Experiment: particle chemistry, shape, mixing state and complex refractive index, Tellus B, 63, 475-496, 2011.
Kang, S., Hwang, H., Kang, S., Park, Y., Kim, H., and Ro, C.-U.: Quantitative ED-EPMA combined with morphological information for the characterization of individual aerosol particles collected in Incheon, Korea, Atmospheric Environment, 43, 3445-3453, 2009.
Kaspari, S., Painter, T. H., Gysel, M., Skiles, S. M., and Schwikowski, M.: Seasonal and elevational variations of black carbon and dust in snow and ice in the Solu-Khumbu, Nepal and estimated radiative forcings, Atmos. Chem. Phys., 14, 8089–8103, doi:10.5194/acp-14- 8089-2014, 2014.
~~Kaspari, S., Painter, T., Gysel, M., and Schwikowski, M.: Seasonal and elevational variations of black carbon and dust in snow and ice in the Solu Khumbu, Nepal and estimated radiative forcings, Atmospheric Chemistry and Physics Discussions, 13, 33491-33521, 2013.~~
Kerker, M., Scheiner, P., Cooke, D., and Kratohvil, J.: Absorption index and color of colloidal hematite, Journal of Colloid and Interface Science, 71, 176-187, 1979.
Kim, D., Chin, M., Yu, H., Eck, T. F., Sinyuk, A., Smirnov, A., and Holben, B.: Dust optical properties over North Africa and Arabian Peninsula derived from the AERONET dataset, Atmos. Chem. Phys., 11(20), 10733-10741, 2011.
Klaver, A., Formenti, P., Caquineau, S., Chevaillier, S., Ausset, P., Calzolai, G., Osborne, S., Johnson, B., Harrison, M., and Dubovik, O.: Physico - chemical and optical properties of Sahelian and Saharan mineral dust: in situ measurements during the GERBILS campaign, Quarterly Journal of the Royal Meteorological Society, 137, 1193-1210, 2011a.
Klaver, Y., Lemmens, V., Creemers, G., Rutten, H., Nienhuijs, S., and de Hingh, I.: Population-based survival of patients with peritoneal carcinomatosis from colorectal origin in the era of increasing use of palliative chemotherapy, Annals of oncology, 22, 2250-2256, 2011b.
Koven, C. D., and Fung, I.: Inferring dust composition from wavelength-dependent absorption in Aerosol Robotic Network (AERONET) data, Journal of Geophysical Research: Atmospheres

(1984 – 2012), 111, 2006.
Köhler, C. H., Trautmann, T., Lindermeir, E., Vreeling, W., Lieke, K., Kandler, K., Weinzierl, B., Groß, S., Tesche, M., and Wendisch, M.: Thermal IR radiative properties of mixed mineral dust and biomass aerosol during SAMUM – 2, Tellus B, 63, 751-769, 2011.
Krekov, G. M.: Models of atmospheric aerosols, in Aerosol Effects on Climate, edited by S. G. Jennings, Univ. of Ariz. Press, Tucson, 9-72, 1992.
Lázaro, F. J., Gutiérrez, L., Barrón, V., and Gelado, M. D.: The speciation of iron in desert dust collected in Gran Canaria (Canary Islands): Combined chemical, magnetic and optical analysis, Atmospheric Environment, 42, 8987-8996, 2008.
Lack, D. A., Quinn, P. K., Massoli, P., Bates, T. S., Coffman, D., Covert, D. S., Sierau, B., Tucker, S., Baynard, T., Lovejoy, E., Murphy, D. M., and Ravishankara, A. R.: Relative humidity dependence of light absorption by mineral dust after long-range atmospheric transport from the Sahara, Geophys. Res. Lett., 36, L24805, doi:10.1029/2009GL041002, 2009.
Lafon, M., Megret, F., Lafage, M., and Prehaud, C.: The innate immune facet of brain, Journal of molecular neuroscience, 29, 185-194, 2006.
Lafon, S., Rajot, J.-L., Alfaro, S. C., and Gaudichet, A.: Quantification of iron oxides in desert aerosol, Atmospheric Environment, 38, 1211-1218, 2004.
Lawrence, C. R., Painter, T., Landry, C., and Neff, J.: Contemporary geochemical composition and flux of aeolian dust to the San Juan Mountains, Colorado, United States, Journal of Geophysical Research: Biogeosciences (2005–2012), 115, 2010.
Levoni, C., Cervino, M., Guzzi, R., and Torricella, F.: Atmospheric aerosol optical properties: a database of radiative characteristics for different components and classes, Applied optics, 36, 8031-8041, 1997.
Liao, H., Seinfeld, J. H.: Radiative forcing by mineral dust aerosols: sensitivity to key variables, J. Geophys. Res.-Atmos., 103(D24), 31637-31645,doi:10.1029/1998JD200036, 1998.
Linke, C., Möhler, O., Veres, A., Mohacsi, A., Bozóki, Z., Szabó, G., and Schnaiter, M.: Optical properties and mineralogical composition of different Saharan mineral dust samples: a laboratory study, Atmospheric Chemistry and Physics, 6, 3315-3323, 2006a.
~~Linke, D., Riess, T., Autenrieth, I. B., Lupas, A., and Kempf, V. A.: Trimeric autotransporter adhesins: variable structure, common function, Trends in microbiology, 14, 264-270, 2006b.~~
Longtin, D. R., Shettle, E. P., Hummel, J. R., and Pryce, J. D.: A wind dependent desert aerosol model: Radiative properties, Air Force Geophys. Lab., Air Force Syst. Command Hanscom Air Force Base, Mass, AFGL-TR-88-0112, 115, 1988.
Lu H., Wei W., Liu M., Wu X., Mou S., and Han Q.: Quantification and semi-quantification of iron-oxide Minerals in Aerosol Particles in the Hinterland of Taklimakan Desert. SCIENTIA GEOGRAPHICA SINICA, 31, 969-975, 2011.
~~Müller T., Schladitz A., Massling A., Kaaden N., Kandler K., and Wiedensohler A.: Spectral absorption coefficients and imaginary parts of refractive indices of Saharan dust during SAMUM-1, Tellus B, 61, 79-95, 2009.~~
Mahowald, N., Albani, S., Kok, J. F., Engelstaeder, S., Scanza, R., Ward, D. S., and Flanner, M. G.: The size distribution of desert dust aerosols and its impact on the Earth system, Aeolian Research, 2013.
Malek, M. A., Kim, B., Jung, H.-J., Song, Y.-C., and Ro, C.-U.: Single-particle mineralogy of Chinese soil particles by the combined use of low-Z particle electron probe X-ray microanalysis and attenuated total reflectance-FT-IR imaging techniques, Analytical chemistry, 83, 7970-7977, 2011.

Marra, A., Blanco, A., Fonti, S., Jurewicz, A., and Orofino, V.: Fine hematite particles of Martian interest: absorption spectra and optical constants, Journal of Physics: Conference Series, 2005, 132.

McConnell, C., Formenti, P., Highwood, E., and Harrison, M.: Using aircraft measurements to determine the refractive index of Saharan dust during the DODO Experiments, Atmospheric Chemistry and Physics, 10, 3081-3098, 2010.

Meland, B., Kleiber, P., Grassian, V., and Young, M.: Visible light scattering study at 470, 550, and 660nm of components of mineral dust aerosol: Hematite and goethite, Journal of Quantitative Spectroscopy and Radiative Transfer, 112, 1108-1118, 2011.

Menéndez, I., Pérez-Chacón, E., Mangas, J., Tauler, E., Engelbrecht, J. P., Derbyshire, E., Cana, L., and Alonso, I.: Dust deposits on La Graciosa Island (Canary Islands, Spain): Texture, mineralogy and a case study of recent dust plume transport, Catena, 117, 133-144, 2014.

Mishchenko, M. I., Travis, L. D., and Lacis, A. A.: Scattering, absorption, and emission of light by small particles, Cambridge university press, 2002.

Mishra, S., Tripathi, S., Aggarwal, S. G., and Arola, A.: Optical properties of accumulation mode, polluted mineral dust: effects of particle shape, hematite content and semi-external mixing with carbonaceous species, Tellus B, 64, 2012.

Mishra, S. K., and Tripathi, S.: Modeling optical properties of mineral dust over the Indian Desert, Journal of Geophysical Research: Atmospheres (1984–2012), 113, 2008.

Moosmüller, H., Engelbrecht, J. P., Skiba, M., Frey, G., Chakrabarty, R. K., and Arnott, W. P.: Single scattering albedo of fine mineral dust aerosols controlled by iron concentration, Journal of Geophysical Research: Atmospheres (1984–2012), 117, 2012.

Mukai, T.: Cometary dust and interplanetary particles, Evolution of interstellar dust and related topics, 1989, 397.

Müller T., Schladitz A., Massling A., Kaaden N., Kandler K., and Wiedensohler A.: Spectral absorption coefficients and imaginary parts of refractive indices of Saharan dust during SAMUM-1, Tellus B, 61, 79-95, 2009.~~Muller~~

Müller, T., Schladitz, A., Kandler, K., and Wiedensohler, A.: Spectral particle absorption coefficients, single scattering albedos and imaginary parts of refractive indices from ground based in situ measurements at Cape Verde Island during SAMUM-2, Tellus B, 63(4), 573-588, 2011.

Muñoz, O., Volten, H., Hovenier, J., Min, M., Shkuratov, Y. G., Jalava, J., Van der Zande, W., and Waters, L.: Experimental and computational study of light scattering by irregular particles with extreme refractive indices: hematite and rutile, 2006.

Nickovic, S., Vukovic, A., Vujadinovic, M., Djurdjevic, V., and Pejanovic, G.: Technical Note: High-resolution mineralogical database of dust-productive soils for atmospheric dust modeling, Atmospheric Chemistry and Physics, 12, 845-855, 2012.

Nickovic, S., Vukovic, A., and Vujadinovic, M.: Atmospheric processing of iron carried by mineral dust, Atmospheric Chemistry and Physics, 13, 9169-9181, 2013.

Onari, S., Arai, T., and Kudo, K.: Infrared lattice vibrations and dielectric dispersion in α-Fe 2 O 3, Physical Review B, 16, 1717, 1977.

Osborne, S. R., Johnson, B. T., Haywood, J. M., Baran, A. J., Harrison M. A. J., and McConnell, C. L.: Physical and optical properties of mineral dust aerosol during the Dust and Biomass-burning Experiment, J. Geophys. Res.-Atmos., 113, D00C03, doi:10.1029/2007JD009551, 2008.

Otto, S., Bierwirth, E., Weinzierl, B., Kandler, K., Esselborn, M., Tesche, M., Schladitz, A., Wendisch, M., and Trautmann, T.: Solar radiative effects of a Saharan dust plume observed during SAMUM

assuming spheroidal model particles, Tellus B, 61, 270-296, 2009.
Painter, T. H., Deems, J. S., Belnap, J., Hamlet, A. F., Landry, C. C., and Udall, B.: Response of Colorado River runoff to dust radiative forcing in snow, Proceedings of the National Academy of Sciences, 107, 17125-17130, 2010.
Patterson, E., and Gillette, D.: Commonalities in measured size distributions for aerosols having a soil - derived component, Journal of Geophysical Research, 82, 2074-2082, 1977.
Peterson, J. T.: Measurement of atmospheric aerosols and infrared radiation over Northwest India and their relationship, DTIC Document, 1968.
Petzold, A., Rasp, K., Weinzierl, B., Esselborn, M., Hamburger, T., Dörnbrack, A., Kandler, K., Schütz, L., Knippertz, P., and Fiebig, M.: Saharan dust absorption and refractive index from aircraft - based observations during SAMUM 2006, Tellus B, 61, 118-130, 2009.
Petzold, A., Veira, A., Mund, S., Esselborn, M., Kiemle, C., Weinzierl, B., Hamburger, T., Ehret, G., Lieke, K., and Kandler, K.: Mixing of mineral dust with urban pollution aerosol over Dakar (Senegal): impact on dust physico-chemical and radiative properties, Tellus B, 63(4), 619-634, 2011.
Popova, S., Tolstykh, T., and Ivlev, L.: Optical-Constants of Fe2O3 in infrared spectral region, in MEZHDUNARODNAYA KNIGA DIMITROVA UL., 113095 MOSCOW, RUSSIA, 954-955, 1973.
Postma, D., and Brockenhuus-Schack, B. S.: Diagenesis of iron in proglacial sand deposits of late-and post-Weichselian age, Journal of Sedimentary Research, 57, 1987.
Poulton, S. W., and Canfield, D. E.: Development of a sequential extraction procedure for iron: implications for iron partitioning in continentally derived particulates, Chemical Geology, 214, 209-221, 2005.
Qin, Y., and Mitchell, R.: Characterisation of episodic aerosol types over the Australian continent, Atmospheric Chemistry and Physics, 9, 1943-1956, 2009.
Querry, M. R.: Optical constants of minerals and other materials from the millimeter to the ultraviolet, DTIC Document, 1987.
Querry, M. R., Osborne, G., Lies, K., Jordon, R., and Coveney Jr, R. M.: Complex refractive index of limestone in the visible and infrared, Applied optics, 17, 353-356, 1978.
Querry, M. R.: Optical constants, Aberdeen Proving Ground, MD 21001, US Army Chemical Research and Development Center (CRDC), 418, 1985.
Raiswell, R., and Anderson, T.: Reactive iron enrichment in sediments deposited beneath euxinic bottom waters: constraints on supply by shelf recycling, Geological Society, London, Special Publications, 248, 179-194, 2005.
Redmond, H. E., Dial, K. D., and Thompson, J. E.: Light scattering and absorption by wind blown dust: Theory, measurement, and recent data, Aeolian Research, 2, 5-26, 2010.
Reynolds, R. L., Goldstein, H. L., Moskowitz, B. M., Bryant, A. C., Skiles, S. M., Kokaly, R. F., Flagg, C. B., Yauk, K., Berquó, T., and Breit, G.: Composition of dust deposited to snow cover in the Wasatch Range (Utah, USA): Controls on radiative properties of snow cover and comparison to some dust-source sediments, Aeolian Research, 2013.
Reynolds, R. L., Cattle, S. R., Moskowitz, B. M., Goldstein, H. L., Yauk, K., Flagg, C. B., Berquó, T. S., Kokaly, R. F., Morman, S., and Breit, G. N.: Iron oxide minerals in dust of the Red Dawn event in eastern Australia, September 2009, Aeolian Research, 2014.
Ryder, C. L., Highwood, E. J., Rosenberg, P. D., Trembath J., Brooke, J. K., Bart, M., Dean, A.,

Crosier, J., Dorsey, J., Brindley, H., Banks, J., Marsham, J. H., McQuaid, J. B., Sodemann, H., and Washington, R.: Optical properties of Saharan dust aerosol and contribution from the coarse mode as measured during the Fennec 2011 aircraft campaign, Atmos. Chem. Phys., 13(1), 303-325, 2013.

Scanza, R., Mahowald, N., Ghan, S., Zender, C., Kok, J., Liu, X., Zhang, Y., Yu, S., Mathur, R., and Pleim, J.: Modeling dust as component minerals in the Community Atmosphere Model: development of framework and impact on radiative forcing, Atmos. Chem. Phys, 14, 11247-11285, 2014.

Scheinost, A., Chavernas, A., Barrón, V., and Torrent, J.: Use and limitations of second-derivative diffuse reflectance spectroscopy in the visible to near-infrared range to identify and quantity fe oxide minerals in soils, Clays and Clay Minerals, 46, 528-536, 1998.

Scheuvens, D., Kandler, K., Küpper, M., Lieke, K., Zorn, S., Ebert, M., Schütz, L., and Weinbruch, S.: Individual - particle analysis of airborne dust samples collected over Morocco in 2006 during SAMUM 1, Tellus B, 63, 512-530, 2011.

Schladitz, A., Müller, T., Kaaden, N., Massling, A., Kandler, K., Ebert, M., Weinbruch, S., Deutscher, C., and Wiedensohler, A.: In situ measurements of optical properties at Tinfou (Morocco) during the Saharan Mineral Dust Experiment SAMUM 2006, Tellus B, 61, 64-78, 2009.

Schroth, A. W., Crusius, J., Sholkovitz, E. R., and Bostick, B. C.: Iron solubility driven by speciation in dust sources to the ocean, Nature Geoscience, 2, 337-340, 2009.

Schwertmann, U.: Relations between iron oxides, soil color, and soil formation, Soil color, 51-69, 1993.

Shao, Y., Wyrwoll, K.-H., Chappell, A., Huang, J., Lin, Z., McTainsh, G. H., Mikami, M., Tanaka, T. Y., Wang, X., and Yoon, S.: Dust cycle: An emerging core theme in Earth system science, Aeolian Research, 2, 181-204, 2011.

Shen, Z., Cao, J., Zhang, X., Arimoto, R., Ji, J., Balsam, W., Wang, Y., Zhang, R., and Li, X.: Spectroscopic analysis of iron-oxide minerals in aerosol particles from northern China, Science of the total environment, 367, 899-907, 2006.

Shettle, E. P., and Fenn, R. W.: Models for the aerosols of the lower atmosphere and the effects of humidity variations on their optical properties, DTIC Document, 1979.

Shi, Z., Shao, L., Jones, T., and Lu, S.: Microscopy and mineralogy of airborne particles collected during severe dust storm episodes in Beijing, China, Journal of Geophysical Research: Atmospheres (1984–2012), 110, 2005.

Shi, Z., Krom, M. D., Bonneville, S., Baker, A. R., Jickells, T. D., and Benning, L. G.: Formation of iron nanoparticles and increase in iron reactivity in mineral dust during simulated cloud processing, Environmental science & technology, 43, 6592-6596, 2009.

Shi, Z., Bonneville, S., Krom, M., Carslaw, K., Jickells, T., Baker, A., and Benning, L. G.: Iron dissolution kinetics of mineral dust at low pH during simulated atmospheric processing, Atmospheric Chemistry and Physics, 11, 995-1007, 2011.

Shi, Z., Krom, M. D., Jickells, T. D., Bonneville, S., Carslaw, K. S., Mihalopoulos, N., Baker, A. R., and Benning, L. G.: Impacts on iron solubility in the mineral dust by processes in the source region and the atmosphere: A review, Aeolian Research, 5, 21-42, 2012.

Smith, A. J., and Grainger, R. G.: Does variation in mineral composition alter the short-wave light scattering properties of desert dust aerosol?, Journal of Quantitative Spectroscopy and Radiative Transfer, 133, 235-243, 2014.

Sokolik, I., Winker, D., Bergametti, G., Gillette, D., Carmichael, G., Kaufman, Y., Gomes, L., Schuetz,

L., and Penner, J.: Introduction to special section: Outstanding problems in quantifying the radiative impacts of mineral dust, Journal of Geophysical Research: Atmospheres (1984–2012), 106, 18015-18027, 2001.

Sokolik, I. N., and Toon, O. B.: Incorporation of mineralogical composition into models of the radiative properties of mineral aerosol from UV to IR wavelengths, Journal of Geophysical Research: Atmospheres (1984–2012), 104, 9423-9444, 1999.

Song, X., and Boily, J.-F.: Carbon dioxide binding at dry FeOOH mineral surfaces: Evidence for structure-controlled speciation, Environmental science & technology, 47, 9241-9248, 2013.

Steyer, T. R.: Infrared optical properties of some solids of possible interest in astronomy and atmospheric physics, 1974.

Sumner, M.: Effect of iron oxides on positive and negative charges in clays and soils, Clay Miner. Bull, 5, 218-226, 1963.

Takahashi, Y., Higashi, M., Furukawa, T., and Mitsunobu, S.: Change of iron species and iron solubility in Asian dust during the long-range transport from western China to Japan, Atmospheric Chemistry and Physics, 11, 11237-11252, 2011.

Takahashi, Y., Furukawa, T., Kanai, Y., Uematsu, M., Zheng, G., and Marcus, M. A.: Seasonal changes in Fe species and soluble Fe concentration in the atmosphere in the Northwest Pacific region based on the analysis of aerosols collected in Tsukuba, Japan, Atmospheric Chemistry and Physics, 13, 7695-7710, 2013.

Tegen, I., Hollrig, P., Chin, M., Fung, I., Jacob, D., and Penner, J.: Contribution of different aerosol species to the global aerosol extinction optical thickness: Estimates from model results, Journal of Geophysical Research: Atmospheres (1984–2012), 102, 23895-23915, 1997.

Thomas, M., and Gautier, C.: Investigations of the March 2006 African dust storm using ground‐based column‐integrated high spectral resolution infrared (8–13 μm) and visible aerosol optical thickness measurements: 2. Mineral aerosol mixture analyses, Journal of Geophysical Research: Atmospheres (1984–2012), 114, 2009.

Tipping, E.: The adsorption of aquatic humic substances by iron oxides, Geochimica et Cosmochimica Acta, 45, 191-199, 1981.

Torrent, J., and Barrón, V.: Diffuse reflectance spectroscopy of iron oxides, Encyclopedia of Surface and Colloid Science, 1438-1446, 2002.

Wagner, R., Ajtai, T., Kandler, K., Lieke, K., Linke, C., Müller, T., Schnaiter, M., and Vragel, M.: Complex refractive indices of Saharan dust samples at visible and near UV wavelengths: a laboratory study, Atmospheric Chemistry and Physics, 12, 2491-2512, 2012.

Wijenayaka, L. A., Rubasinghege, G., Baltrusaitis, J., and Grassian, V. H.: Surface chemistry of α-FeOOH nanorods and microrods with gas-phase nitric acid and water vapor: Insights into the role of particle size, surface structure, and surface hydroxyl groups in the adsorption and reactivity of α-FeOOH with atmospheric gases, The Journal of Physical Chemistry C, 116, 12566-12577, 2012.

Yang S., Sheng Y., Han Y., and Chen S.: Diffuse reflectance spectroscopic analysis of iron-oxide minerals in dust aerosol from Golmud, Journal of Lanzhou University (Natural Sciences), 50, 710-715, 2014.

Zhang, X., Gong, S., Shen, Z., Mei, F., Xi, X., Liu, L., Zhou, Z., Wang, D., Wang, Y., and Cheng, Y.: Characterization of soil dust aerosol in China and its transport and distribution during 2001 ACE‐Asia: 1. Network observations, Journal of Geophysical Research: Atmospheres (1984–2012), 108, 2003.

1073 Zhu, A., Ramanathan, V., Li, F., and Kim D.: Dust plumes over the Pacific, Indian, and Atlantic oceans:
1074 Climatology and radiative impact, J. Geophys. Res.-Atmos., 112, D16208,
1075 doi:10.1029/2007JD008427, 2007.